A Novel Solar Cell Ionotronic Energy Pathway Inspired by an Electric Eel

by

Najiba Soudi

A thesis
presented to the University of Waterloo
in fulfillment of the
thesis requirement for the degree of
Master of Applied Science
in
Electrical and Computer Engineering

Waterloo, Ontario, Canada, 2021

AUTHOR'S DECLARATION

This thesis consists of material all of which I authored or co-authored: see Statement of Contributions included in the thesis. This is a true copy of the thesis, including any required final revisions, as accepted by my examiners.

I understand that my thesis may be made electronically available to the public.

Statement of Contributions

I would like to acknowledge my co-authors who contributed to the research described in this thesis:

- Prof. Sheva Naahidi: Supervision of the research, editing and reviewing papers, providing experimental facilities, providing funding.
- Dr. Navid M.S. Jahed: Providing editorial feedback in the preparation of the individual manuscript in Chapters 2.
- Sama Nanayakkara: Providing editorial feedback in the preparation of the individual manuscript in Chapters 2.

Abstract

Solar cell technology can be one of the best choices for sustainable future energy. Solar energy conversion strategies inspired by nature can play a vital role in solving the significant challenges in solar cell products such as low power conversion efficiency, expensive fabrication process, and materials. In this thesis, we introduce for the first time a solar cell with unique ionotronic technology inspired by an electric eel with a completely novel configuration of hydrogels. This new generation of solar cells utilizes an ionotronic gradient energy pathway which can greatly enhance the efficiency of solar energy collection using mobile ions. This new solar cell is made of a heterogeneous multi-layer hydrogel that mimics the artificial electric eel with the ability to produce relatively large voltage under external stimulation. Device physics, design, fabrication, and optoelectronic characterization of hydrogel solar cell devices are provided in this thesis.

An artificial electrocyte was designed by using polyacrylamide hydrogel synthesized with four different components. The fabricated artificial electrocyte showed 150-180 mV for one cell containing high salinity, cation-selective, low salinity, anion-selective, and high salinity hydrogels. Seven series of these tetrameric gel cells showed 1.27 mV and 2.87 μA by the electromotive force of ionic gradient between low salinity and high salinity gels. By stacking three series gel cells in parallel, about 7 μA is reported. It is shown that the thickness of the gels has a proportional relationship with the resistance of the gels. UV-Vis spectroscopy results show that the high salinity gel is able to absorb light by a maximum peak at 534 nm for 1.5 mm of thickness. The photoconductivity tests prove the designed electric eel-inspired solar cell is able to generate photocurrent. By merging the artificial electrocyte ionic energy pathway and the principles of solar energy converter, the bio-inspired eel solar cell shows 5.08 % power conversion efficiency using three layers of low salinity/high salinity/low salinity hydrogels. The current density of 6.475 mA/cm^2 is obtained for cation-selective/high salinity/anion-selective hydrogel-based solar cell.

For the first time, in this project, not only new materials with exceptional properties have been introduced to the photovoltaic solar systems, but also a novel flexible, eco-friendly solar cell with a unique configuration has been proposed.

Acknowledgements

First of all, I owe a heartfelt gratitude to Professor Sheva Naahidi for all of her support, encouragement and guidance as my supervisor and I would like to thank her for providing me with the opportunity to work in her research group.

Also, I would like to thank Professor Rosenberg for accepting to be my co-supervisor.

A special thanks to Professor Majedi who granted access to his laboratory for research and providing supports through valuable discussions.

In addition, I am truly grateful to Professor Goldthorpe and Professor Safavi-Naeini for reviewing my work, and I appreciate their time and effort to improve the quality of this thesis.

I would like to thank the financial support of Mr. Jeff Peters and providing support through valuable discussions.

I would like to thank Dr. Marwa Abd-Ellah for providing me the access to QNCB533 lab, Mr. Joseph Street, and Dr. Hrilina Gosh for their technical assistance.

Finally, I would like to thank my family and all the people who made this thesis possible.

Dedication

To my family.

Table of Contents

List of Figures……x
List of Tables……..……..…..xii
Chapter 1 Introduction and Objective 1
1.1 Introduction 1
1.2 Thesis Objective 5
1.3 Thesis Outline 6
Chapter 2 Literature Review 7
2.1 Operation Principles of Solar Cells 7
2.2 Bio-inspired Solar Cells 12
2.3 Electric Eel 15
2.4 Hydrogels 19
2.4.1 Conductive Hydrogels 20
2.4.2 Polyacrylamide 22
2.4.3 Synthesis of hydrogels 23
Chapter 3 Materials and Methods 25
3.1 Artificial Electrocyte 25
3.1.1 . Artificial Electrocyte Design Principles 25
3.1.2 Synthesis and Fabrication Process 28
3.1.3 Measurements 29
3.2 Electric Eel Inspired Solar Cell 30
3.2.1 Design Principles 30
3.2.2 Synthesis and Fabrication Process 32
3.2.3 Measurements 32
3.3 Materials 33
Chapter 4 Results and Discussion 35
4.1 Artificial Electrocyte 35
4.1.1 Surface Printed Artificial Electrocyte 36
4.1.2 Fluidic Printed Artificial Electrocyte 39
4.1.3 Design Improvement for Electrical Property Enhancement 45
4.2 Electric-Eel Inspired Solar Cell 48
4.2.1 Light Absorption Properties 49

4.2.2 Photoconductivity Characterizations 53
4.2.3 Solar Simulator Results 57
Chapter 5 Conclusions and Future Prospects 64
5.1 Conclusion 64
5.2 Future Prospects 65
Bibliography 67

List of Figures

Figure 1. Schematic of light interaction with A) macrostructure, B) hierarchical multiscale texture, and C) subwavelength diffraction grating[1]. 10
Figure 2 Primary steps of current generation in organic solar cell 12
Fig. 3. Schematic of typical organisms that inspire solar photovoltaic energy conversion systems[1]. 13
Figure 4 Schematic view of electrocytes in series(Picture adopted from 28 with permission) [28] 16
Figure 5 a. Morphology of an electric eel b. Arrangements of stacked electrocytes and electrocyte structure (Picture adopted from 8 with permission) [8] c. Mechanism of action of voltage generation by depolarization and repolarization(Picture adopted with permission from Animal Physiology Introductory by Sanja Hinic-Frlog-copyright 2019) [31] 18
Figure 6. Different classification of hydrogels 20
Figure 7 Application of conductive hydrogels(Picture adopted from 38 with permission) [38] 22
Figure 8 a. Mechanism of voltage generation in an actual electrocyte. b. Mechanism of voltage generation in an artificial electrocyte 26
Figure 9 Schematic view of the fluidic printed artificial electrocyte, a sequence of high salinity (HS) gel, cation selective (CS) gel, low salinity (LS) gel, and anion selective (AS) gel. Then the pattern repeats starting with a high salinity gel. 27
Figure 10 a. synthesized hydrogels, b. structure of one fluidic printed tetrameric cell, two fluidic printed cells in series, and an arrangement of 6 stacked cells in parallel in which each tube contains three tetrameric cells, and c. the voltage measurement process. 30
Figure 11 Schematic of the electric-eel inspired hydrogel solar cell. 32
Figure 12 a. Electric eel-inspired ionotronic solar cell b. Photoconductivity test, and c. solar simulator test process. 33
Figure 13 Surface printed gel cells a. before and, b. after connection 37
Figure 14 Open circuit voltage of artificial electrocyte as a function of gel volume 37
Figure 15 Open circuit voltage of artificial electrocyte as a function of numbers of gels 38
Figure 16 Surface printed artificial electrocyte after curing and connection 39
Figure 17 Open circuit voltage of fluidic printed artificial electrocyte as a function of curing time of gels 40
Figure 18 Short circuit current of the fluidic printed artificial electrocyte as a function of gel volume 41
Figure 19 Open circuit voltage of the fluidic printed artificial electrocyte as a function of gel volume 42

Figure 20 Internal resistance of gels as a function of thickness 44
Figure 21 Open circuit voltage of the fluidic printed artificial electrocyte with different arrangements ... 45
Figure 22 Open circuit voltage of 7 tetrameric fluidic printed cells 46
Figure 23 Short circuit current of the fluidic printed artificial electrocyte with different arrangements. ... 46
Figure 24 Open circuit voltage of fluidic printed artificial electrocyte as a function of time for a regular and encapsulated sample 48
Figure 25 Absorption spectrum of high salinity gel for 1.5 mm, 3mm, and 6 mm gel thicknesses. 50
Figure 26 UV-Vis spectrum for the cation selective gel, low salinity gel, high salinity gel, and PEDOT:PSS. 52
Figure 27 Absorption spectrum of high salinity gel with red dye and black dye with 1.5 mm thickness. . 53
Figure 28 I-V characteristics of a. anion selective layer and b. high salinity hydrogels in dark and under irradiation 54
Figure 29 a. I-V characteristics of a. low salinity/high salinity hydrogels in dark and under irradiation, b. increase of current under irradiation 54
Figure 30 I-V characteristics of a three layered sample consisting of a layer of high salinity hydrogel sandwiched between anion-selective hydrogel and cation-selective hydrogel in dark and light. 55
Figure 31 I-V behavior of another three layered sample consists of a high salinity hydrogel sandwiched between two layers of low salinity hydrogels in dark and light. 56
Figure 32 I-V characteristics of a five layered sample including low salinity, anion selective, high salinity, and cation selective, and low salinity respectively in dark and light. 57
Figure 33 J-V characteristics of electric eel-inspired solar cell with five layers of high salinity, cation selective, low salinity, and anion selective, and high salinity hydrogels. 58
Figure 34 Characteristics of an electric eel-inspired solar cell with three layers of cation selective, high salinity, and anion selective hydrogels. 59
Figure 35 Characteristics of an electric eel-inspired solar cell with three layers of cation selective, high salinity, and low salinity hydrogels 60
Figure 36 Characteristics of an electric eel-inspired solar cell with two layers of high salinity and low salinity hydrogels. 61
Figure 37 Characteristics of an electric eel-inspired solar cell with three layers of low salinity, high salinity, and low salinity hydrogels 61
Figure 38 Characteristics of an electric eel-inspired solar cell with five layers of low salinity, cation selective, high salinity, and anion selective, and low salinity hydrogels. 62

List of Tables

Table 1. Estimated resistance of the hydrogels of the artificial electrocyte 43
Table 2 Comparison of characteristics between fluidic artificial electrocyte and actual electrocyte 44
Table 3. Performance of different versions of the electric eel-inspired solar cell 62

Chapter 1

Introduction and Objective

1.1 Introduction

Humans' dependency on fossil fuels for thousands of years has resulted in detrimental effects on the planet. Excessive fossil fuel usage has contributed to a significant increase in global temperature since the pre-industrial era [1]. Achieving a low-emission, renewable, and sustainable energy production pathway is the challenge of today's society. Sustainable electricity production is particularly necessary as the United State of America alone consumed 3971 TWh of electricity in 2020[1]. Due to the huge amount of solar energy received every day by the Earth, solar cells are one of the best options for producing electricity sustainably. Assuming this amount is completely converted into electricity by means of conventional solar panels with an average efficiency of 20%, the daily solar power capacity would be 7.2×10^3 TW[1]. Although these calculations are idealized, the daily solar power capacity is 282 times the yearly electricity consumption rate of the world. At the end of 2018, the capacity of global photovoltaic (PV) solar cells surpassed 500 GW and has the potential to be much higher if these systems were more commonplace around the world. By 2030, it is predicted that 3 to 10 TW of solar power can be harnessed [2]. However, in order to compete with existing sources, devices that converts sunlight to electrical energy must be both reliable and cost-effective.

The cost of solar cell manufacturing, energy payback, and feedstock availability are the major barriers to reach efficient large solar modules in order to produce a main portion of the energy need. The dominant solar cells in the PV industry are made of silicon due to their high power

conversion efficiency and durability. Although the single crystal solar cells offer higher efficiency, the production of solar-grade silicon wafers is expensive so these PV cells must be manufactured more economically through technological advances to be a sustainable energy source [3]. To overcome this challenge, various alternatives have been widely investigated during the past decade including organic solar cells, thin-film solar cells, etc. For instance, several industrial solar companies developed thin-film solar cells such as copper indium gallium selenide (CIS/CIGS), amorphous silicon (a-Si), and cadmium telluride (CdTe) to produce less expensive solar technology. These cells contain cost-efficient fabrication procedures and more affordable materials, in comparison with crystalline silicon solar cells [3]. Yet lack of stability and lower power conversion efficiency are the drawbacks of these solar cells. Several attempts have been made recently to enhance the efficiency of low-cost solar cells. For example, organic solar cells have shown near 16% power conversion efficiency however, their unreliable durability makes them distant from the PV market [1].

Despite the efforts that have been done to lower the production cost and improve the efficiency of photovoltaic solar cells, the price per watt of this energy still remains several times greater than that of other resources such as coal, hydroelectric, natural gas, and oil. To abate these limitations, less expensive materials and less complex fabrication processes are needed and it is shown that nature-inspired design can play a major role to lower the manufacturing cost and enhance the efficiency of solar cells. There are several organisms in nature that harvest solar energy like photosynthetic plants which inspired the design of dye sensitized solar cells. Biomimetic photovoltaic solar cells have gained a lot of attention in recent years and have shown significant

improvements in power conversion efficiency. Future photovoltaic solar cells as a sustainable energy resource will rely greatly on novel solutions based on nature-inspired design.

The major steps in harvesting energy through solar energy converters are charge generation by absorption of light, charge carriers' transportation, separation, and collection. Although these steps can be inspired by nature, the subsystems should be designed to maximize performance in an integrated complex system like a bio-inspired solar cell. Expectedly, researchers have been inspired by photosynthetic organisms like plants and some bacteria for improving electron transport [4]. They have also been inspired by a large variety of surface structures from natural organisms, including insect eyes, butterfly wings, and rose petals [5]. Most of the reported inspiration is based on the surface structure of selective or completely anti-reflective surfaces in nature such as moth-eye and butterfly wings [6]. On the other hand, electron transport and collection mechanisms are integral in solar cell design to maximize energy conversion from incoming photons however, the bio-inspired researches mostly focused on light-harvesting techniques [1]. Bio-inspired charge separation and electron-pathway management included in photosynthesis supporting Marcuse's theory on electron transfer lead to the first dye-sensitized solar cell [7]; but several attempts are needed to overcome the challenges in electron transport and collection functionality such as low internal quantum efficiency rate. One novel conceptual bio-inspired strategy is found in electric eels [8]. This project aims to provide a novel, cost-efficient, eco-friendly, and flexible ionotronic electric eel-inspired solar cell in which hydrogels will take part in the energy transport process. At first, we will investigate the reason behind choosing electric-eel as a novel bio-inspiration in the solar energy systems, then we provide our strategy to design the aforementioned novel cell.

An electric-eel is able to generate ~600 V of external electricity from excitable cells [9]. Numerous nanoscale conductors in the cell membrane of the electric organ of an electric-eel effectively trigger and release action potential in the form of ion concentration and act as a battery [9]. The electric organ called the electrocyte[1] in an electrical eel can create 150 mV individually by releasing action potential which is the difference between maximum innervated membrane potential (+65 mV) and non-innervated membrane potential (-85 mV) by the existence of different ion channels and ion pumps [9]. There are thousands of stacked electrocytes [1] in a large electric eel and they can generate 1 A at a short circuit [10]. Ion-selective membrane and asymmetrically ion concentration between the sides make it possible for depolarization and repolarization sequence to happen. Each electrocyte can act as a battery and serial connection between them make an electric eel to be able to create ~600 V to attract prey and ward off predators. A unique strategy that an electric eel uses to generate electrical discharges has been developed at least six times in history for a wide variety of usages such as bio-compatible batteries [8]. A novel electric eel-inspired power concept has been produced recently which can generate 110 V at the open circuit at and the same time they are transparent, biocompatible, durable, and not complicated to manufacture [8]. The capability of such power generation from ion concentration gradients in nano-cells excited by sun irradiation could be a game-changing technology in the future energy market.

[1] Electricity generator organ in an electric eel

1.2 Thesis Objective

As it is discussed in the previous section, it is essential to find a renewable energy source due to the limited number of fossil fuel sources. In this regard, implementing a sustainable energy resource is highly demanded. A huge amount of solar energy is received every day by the Earth, while it is pervasively existing, the solar cell is probably one of the best choices for sustainable future energy necessities [11]. On the other hand, many sustainable engineering management solutions are successfully adapted from nature [3]. Bioinspired photonics is the study of organisms and natural mechanisms and structures that have the ability to generate, detect and control light or enhance the optical properties of materials. A new generation of bio-inspired solar technology is proposed here for the first time by merging electric eel ionic energy pathways and dye-sensitized solar cell technology. The material and the configuration of each layers are completely novel. To innovate this unique solar cell, at first, an artificial electrocyte has been created by mimicking the electric eel's mechanism of action to produce external different potential by ionic gradient from excitable internal cells. The next step can be a feasibility study over the design of an ideal photovoltaic solar cell based on the combination of low-cost materials, light absorbers, and electrical circuits to collect photovoltage/photocurrent. An environmentally friendly, efficient, flexible, and semi-transparent novel solar cell is proposed by mimicking the electric-eel mechanism of action. To design the artificial electrocyte, polyacrylamide hydrogels can be utilized in four different concentrations of components. Then, the artificial electrocyte's design can be developed by mimicking the properties of the selective ion channels in the cell membrane of the electrocyte. The cell may include high salinity gel as extracellular space, low salinity gel as intracellular space, and cation and anion-selective gels as membranes. After optimizing the

hydrogel synthesis process, the electric eel-inspired solar cell should be designed. The high salinity layer can act as an active layer with the ability to generate photocurrent, while low salinity layers can act as receptors in this cell.

In this project, the number one goal is finding a new and cost-efficient material with desirable properties to fulfill the requirements of photovoltaic solar systems. In addition, I aim to design a novel flexible and semi-transparent solar cell with a unique configuration which is eco-friendly and inexpensive.

1.3 Thesis Outline

In this thesis, the second chapter reviews the recent advances in solar cells, electric-eel inspired electronics, and the application of hydrogels. In addition, the principles of each concept have been provided. Chapter three provides the information about designing, fabrication, and measurements of the artificial electrocyte and the electric-eel-inspired solar cell. Chapter four reports the effect of gel thickness, cell arrangements, and stacking of gels on the current, voltage, and resistance features of the artificial electrocyte. In the second part of the results, the characteristics of the electric-eel inspired solar cell are reported. The UV-Vis spectrum, photoconductivity results, and I-V characteristics under one sun irradiation have been reported. Finally, in chapter five, the summary of the thesis and the future prospects of this project are provided.

Chapter 2

Literature Review

2.1 Operation Principles of Solar Cells

Solar energy conversion originated from Jan Ingenhousz's hypothesis in 1779[3]. Jan based this concept on Joseph Priestley's cylinder created in 1771 which was inspired by photosynthesis, a process used to sustain life on earth for 3.5 billion years. The first photovoltaic observation was conducted in 1839 by Becquerel through investigation of electrolytic cells and the effect of light on them[13]. More than a century passed before the first silicon solar cell was developed in Bell Labs. In 1954, Chapin and Fuller developed the first silicon PV cell which was capable of converting sunlight to electricity with 4% efficiency. In the 1960s, pivotal concepts including thin-film technology, polycrystalline silicon, and compound semiconductor solar cells were developed[14]. The energy demand in 1970 encouraged researchers to develop more efficient and cost-effective solar cells[5]. Tang (1986), demonstrated the first type of organic solar cell with a conversion efficiency of 1%. Organic solar cells report 17% photo conversion efficiency today[5]. O'Regan and Gratzel created the first Gratzel cell or dye-sensitized solar cells (DSSC) whose mechanism mimics that of natural photosynthesis in 1991[15]. In photosynthesis, the antenna complex and photosynthetic reaction center proteins (RCs) perform light harvesting and charge separation. In the DSSC, the antenna complex and RCs are replaced by a dye and semiconductor. Todays' DSSCs are low-cost solar energy converters, which have reached a power conversion efficiency up to 12%[11]. Perovskite solar cells are a more recent development which can reach a power conversion efficiency of 21%. The National Renewable Energy Laboratory reports that the

conversion efficiency of both organic and inorganic solar cells has increased from 4% in the first solar cell to 28.8% in GaAs solar cells today[16]. The growing concern of finding green energy sources is creating a large demand for eco-friendly solar cell products.

Solar cells create current and voltage using external optical power without relying on an internal power supply. The difference of energy dissipates in the form of heat[17]. There are several parameters that play key roles in solar cells performance in generation of high current. For instance, active layer light absorption property has a vital effect on the current generation. Active layer transforms the light into charge carriers which generates electrical current for an external low via free charge carriers transportation and collection.

In general, to maintain a proper current density in any type of solar cells, four spate processes must take place. First step is photon absorption in active layer. So, it is crucial to examine the active layer's quality to absorb light and consideration of material properties such as band gap, energy levels in organic semiconductors, and energy coordination of donor and acceptor agents. Second step is formation of free charge carries in the active layer including electron/hole pairs. After generation of free charge carriers, transportation of the excitons from active layer to electron transport layer and hole transport layer is necessary. At final step, the dissociate charge carriers should be collected by electrodes[18].

Since photovoltaic solar systems create electricity for external loads, obstructing any of the foregoing processes reduces the size of the extracted current, resulting in poor device performance[19]. In order to have high performance, the absorbed photons should be a larger portion of the incoming incident light and the dissociated charge carriers should be successfully

collected. If the absorbed photons are not able to generate a large number of free charge carriers, the photocurrent will be very low. Similarly, the efficiency of the solar cell will be low if the free charge carries couldn't transport, dissociate and collected properly. In the following paragraphs, light absorption enhancement technics as well as electron transport mechanisms are discussed in more details.

The primary step in any kind of solar device is light absorption; therefore, maximizing panchromatic light collection is fundamental to improving solar cell efficiency. In semiconductor active layers, it is fair to say that photons with energies less than the semiconductor band gap, no electron hole pair is created which is the key step to generate photocurrent. On the other hand, photos with energy level higher than the band gap energy, form electron hole pairs which are required to current flow at external load[20].

The three principles relevant to improving light harvesting are light coupling at the initial contact surface, light trapping in weakly absorbed wavelength regions, and the removal of optical losses. The main mechanisms for collecting incident light are anti-reflective coatings based on subwavelength surface structures (See Fig. 1.C) and a light trapping strategy by hierarchical nano/microscale textures (See Fig. 1.B)[12].

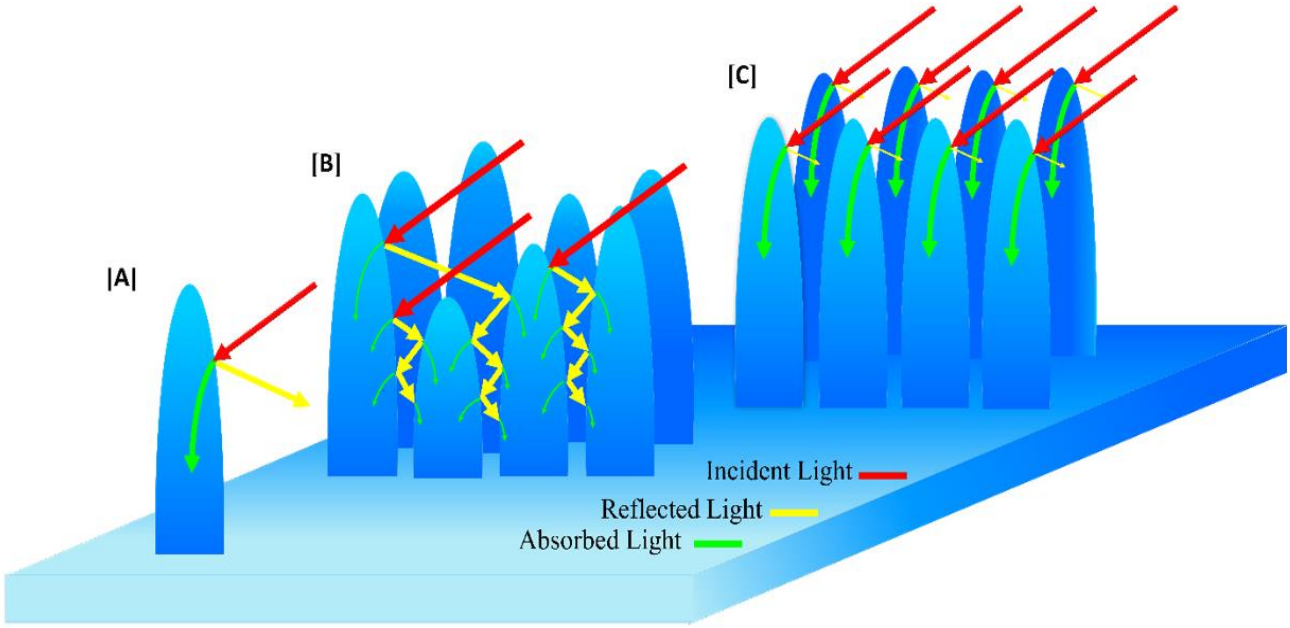

Figure 1. Schematic of light interaction with A) macrostructure, B) hierarchical multiscale texture, and C) subwavelength diffraction grating[1].

Once incident light is absorbed by the active layers in solar cells, the photogenerated carriers have to be transported, dissociated, and collected through the device electrodes [7]. Fundamentally, the collection, separation and transport of electrons/hole pairs prior to their recombination in semiconductor solar cells (including junctions, interfaces and quantum-confined structures is an inefficient process [7]. Except for dye sensitized solar cells where the absorbed energy of photons are transferred to ionic systems, the quantum efficiency of all solar cells drops significantly in these steps due, among just a few factors, to thermalization, loss-in-potential and carrier diffusion [14]. In fact, the dye sensitized solar cell is inspired by photosynthesis in nature where all PV processes are handled separately by different materials and combined ion/electron systems, recently denoted as ionotronic systems [14-15]. Exciton migration is the key point of energy transfer in solar cells. The electron/hole pairs must migrate and reach the interface of

electron transport and hole transport layers in order to dissociate. Excitons are meta-stable and they will expire as soon as their minority carrier lifetime. After this time, free electrons and holes will recombine and in this way, the electro/hole pair will be lost. In order to improve the overcome this challenge, bulk heterojunction solar cells have been developed[21]. By reducing the length of electron/hole transportation path, the chance of recombination before dissociation reduces.

Dissociation of the electron/hole pair happens once the free charge carriers reach the interface of active layer and electron transport layer and hole transport layer. A p-n junction prevents the recombination to happen and leads the electron hole pair to separate. This separation happens by electric field at p-n junction. If the minority carriers get to the junction, the charge carrier swept across the interface and it turns to be large majority carriers in the new layer[22]. Finally, the carriers get collected by electrodes and flow through the circuit. Fig.2 shows the primary steps of current generation in solar cells. To enhance the performance of charge collection in solar cells, transport layers have been developed recently. Electron transport layer adds another junction to the structure of solar cells and will collect the electrons before recombination due to its lower fermi level compared to the active layer. For hole transport layer, the holes get collected before recombination due to its higher fermi level regarding to the active layer[23]. These layers enhance the photo stability of solar cell in turn, the power conversion efficiency of the solar cell.

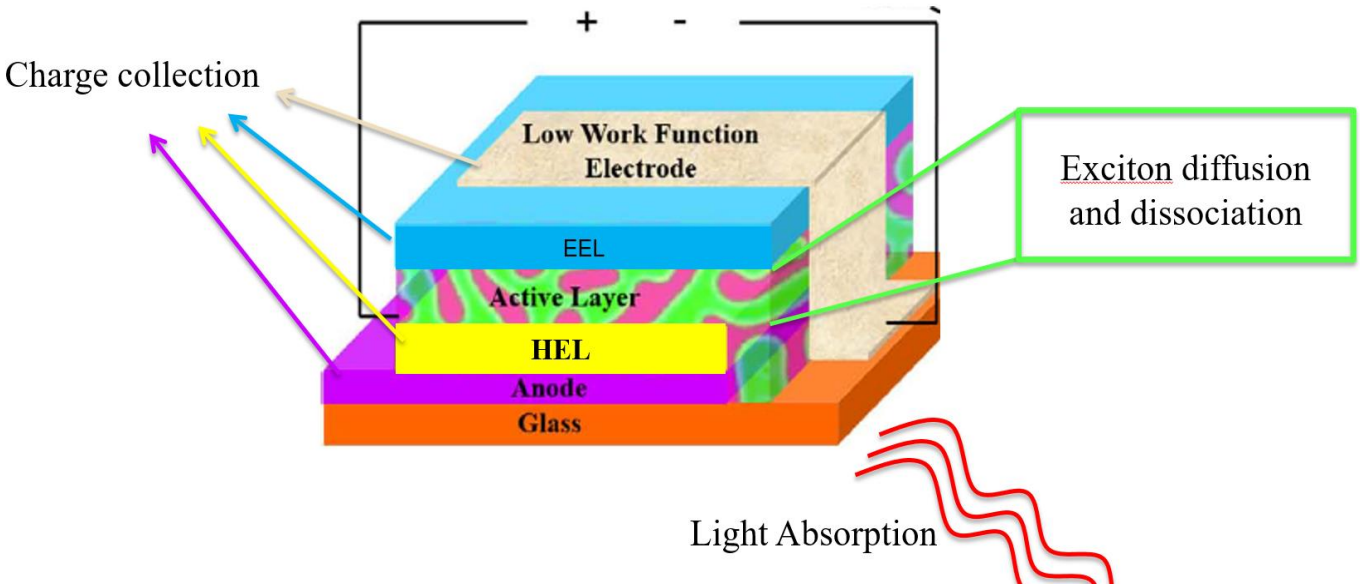

Figure 2 Primary steps of current generation in organic solar cell

2.2 Bio-inspired Solar Cells

Over the last several decades, significant research efforts have been made on bio-inspired solar cells. More research is underway to improve the efficiency of all types of solar cells. Surface morphology of natural organisms can inspire innovative surface coatings that maximize light absorption. Several insects, plants, and other organisms have anatomical features that have evolved to focus light or reduce reflection[5]. Some of these features were meant to improve camouflage or attract mates, while others use their surface structures to maximize energy production through photosynthesis[1]. These traits are important to consider when searching for organisms that may have useful structures or mechanisms. A common theme is the use of tapered shapes like cones to gradually change refractive indices, as seen from the multitude of moth-eye or butterfly wing inspired structures. Another commonality is the presence of 2D arrays of holes that allow certain wavelengths to pass through the material and block all other wavelengths, as found in butterfly

wings and human teeth. The more random and complex the surface structure is, the more successful it is at harvesting light. However, complicated surface films are more difficult and expensive to manufacture and can lead to increased charge recombination[1]. Fig. 1-3 presents a schematic of typical organisms that have inspired different types of solar cells.

Fig. 3. Schematic of typical organisms that inspire solar photovoltaic energy conversion systems[1].

Two particular characteristics of bioinspired photonics, structural color and light harvesting antennas in photosynthetic organisms, are applicable to solar cell technologies, mostly as applied to dye sensitized devices [10-11]. One proposed method for enhancing light capture is to mimic structures in nature, which are optimized for light absorption. Biological organisms have optimized

optical structures over millions of years to attract mates and to camouflage. The main possible inspirations for solar cell design are from insects and plants. Many insects have intricate surface structures that reflect minimal light. All plants absorb light to convert to usable energy, and some have optimized the process for their specific environmental conditions[1].

Electron transport and collection mechanisms are integral in solar cell design to maximize energy conversion from incoming photons. Excitation energy from the absorption of incident light creates electron-hole pairs, which can then be captured by electrodes. The goal is to create as many charges as possible from the energy of the incoming photons and then efficiently collect them. There are some features that play vital roles in the enhancement of charge transport efficiency including the yield of electron injection, the diffusion coefficients, redox reactions, and electron communication. Photosynthetic organisms achieve electron-transfer with almost 100%. Consequently, photosynthesis has inspired an entire category of solar cells, DSSCs. Research on charge separation, transfer of electrons, and electron collection in solar cells can improve efficiency in solar energy converters[1].

Autotrophs like plants and photosynthetic bacteria use sunlight to produce their energy supply, and have optimized electron transfer and collection. Bio-inspired charge separation and electron-pathway management included in photosynthesis have yielded surprising results when applied in solar cells supporting Marcuse's theory on electron transfer[15]. The design of the morphology of the electron transport layer, planar or mesoporous, the geometry of donor/acceptor and the redox potential can be optimized to minimize charge loss, recombination rate and reorganization of energy[1]. The use of bio-inspired dyes in DSSCs has dominated research due to their reduced impact on the environment and cost effectiveness. Several studies have shown that bio-inspired

dye sensitizers are often not as effective nor as long-lasting as Ruthenium dyes[16]. In summary, a combination of nature-inspired designs and the use of modified materials in conventional methods can lead to the production of highly efficient, cost-effective, and environmentally-friendly solar cells. This involves improvements to light-harvesting techniques and enhancement of power conversion efficiency. Remarkable efforts are needed to overcome major concerns of the fabrication and implementation of materials to be sustainable.

2.3 Electric Eel

Electric eels generate bioelectricity by employing flattened cells called electroplaques to travel, interact, defend and hunt. An electric-eel is able to generate ~600 V of external electricity from excitable cells[9]. Numerous nanoscale conductors in the cell membrane of the electric organ of electric-eel effectively trigger and release action potential in the form of ion concentration and act as a battery[25]. There are thousands of stacked electrocytes in a large electric eel and they can generate about 600 V and 1 A at a short circuit. Transmembrane proteins differ between innervated and non-innervated layers. The positive innervated layer with respect to the non-innervated layer caused by depolarization across the membrane in response to impulses leads to the ionic concentration gradient across the cell membrane of electrocyte[26]. Ion-selective membrane and asymmetrically ion concentration between the sides make it possible for depolarization and repolarization sequence to happen. Numerous nanoscale conductors in the cell membrane of the electric organ of electric eel play critical roles to effectively trigger and release action potential in the form of ion concentration[27]. The electric organ called the electrocyte in electrical eel can create 150 mV individually by releasing action potential which is the difference between maximum

innervated membrane potential and non-innervated membrane potential by the existence of different ion channels and ion pumps. Each electrocyte can act as a battery and serial connection between them make electric eel to be able to create ~600 V to attract prey and ward off predators. In other words, each electrocyte act as a battery and by stacking these little batteries, a huge different potential and electric current are generated (see Fig. 4).

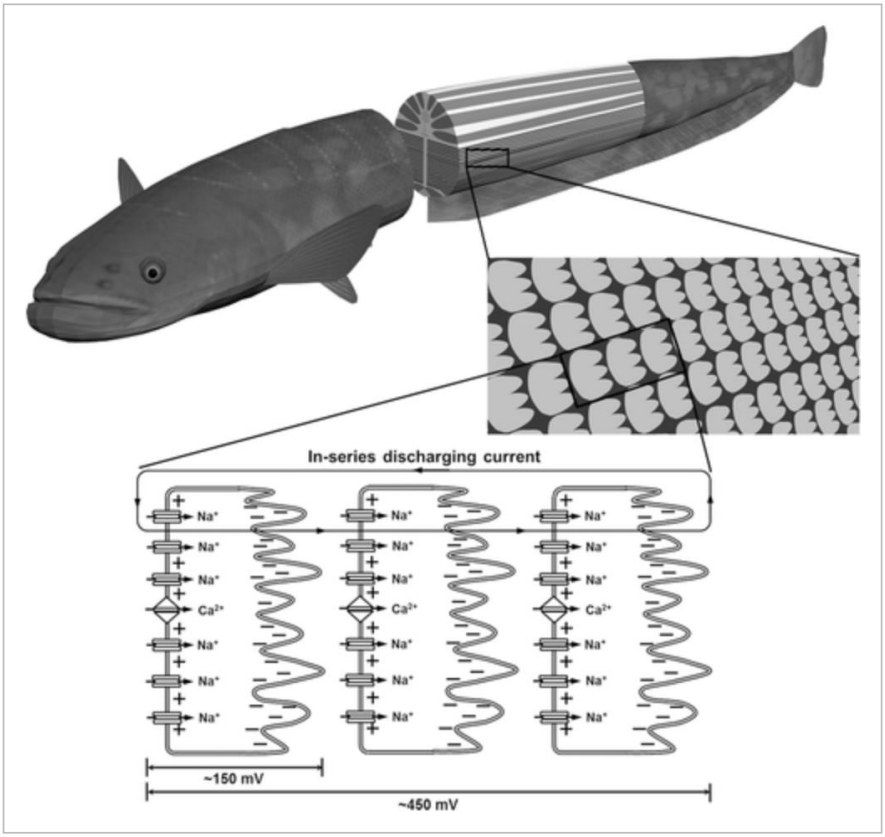

Figure 4 Schematic view of electrocytes in series(Picture adopted from 28 with permission) [28]

An electric eel has three specified organs that make it possible to create ~600 V shock to predators or prays. These organs called Hunter's organ, Sach's organ and the Main organ. These organs make up three quarters of an electric eel's body. These organs are made from electrocytes

and transmit various frequencies of electric signals. The Hunter and Main organs are responsible to produce high voltage for purposes like hunting and Sach's organ is responsible to generate low voltages. Electrocytes are muscle like cells and they are attached to the axons[29]. As soon as the electric eel locates the prey, nerve signals are released from the brain to the electrocytes. Then, electrocytes simultaneously open the Na+ ion channel.

Generally, there are high concentration of sodium ions in the extracellular space than intracellular space. On the other hand, the concentration of potassium ions is higher at the intracellular space. There are also calcium ions in both intra and extra cellular space[30]. At the resting mode, the different potential between intracellular and extracellular space in an electrocyte is -85 mV. By receiving the nerve signals, the sodium ion channels which are selective nano channels get opened and there is a flow of sodium ions toward the intracellular space due to osmotic force. In this step, the cell is depolarizing. The depolarization continues until the different potential between extracellular space and intracellular space is +65 mV. By energy obtained from the hydrolysis, the ATPase will sustain the resting potential by repolarization. The potassium selective ion channels open and the difference potential between exterior membrane and interior membrane gets to -85mV again by potassium ion flow from intracellular space to extracellular space (See Fig. 5).

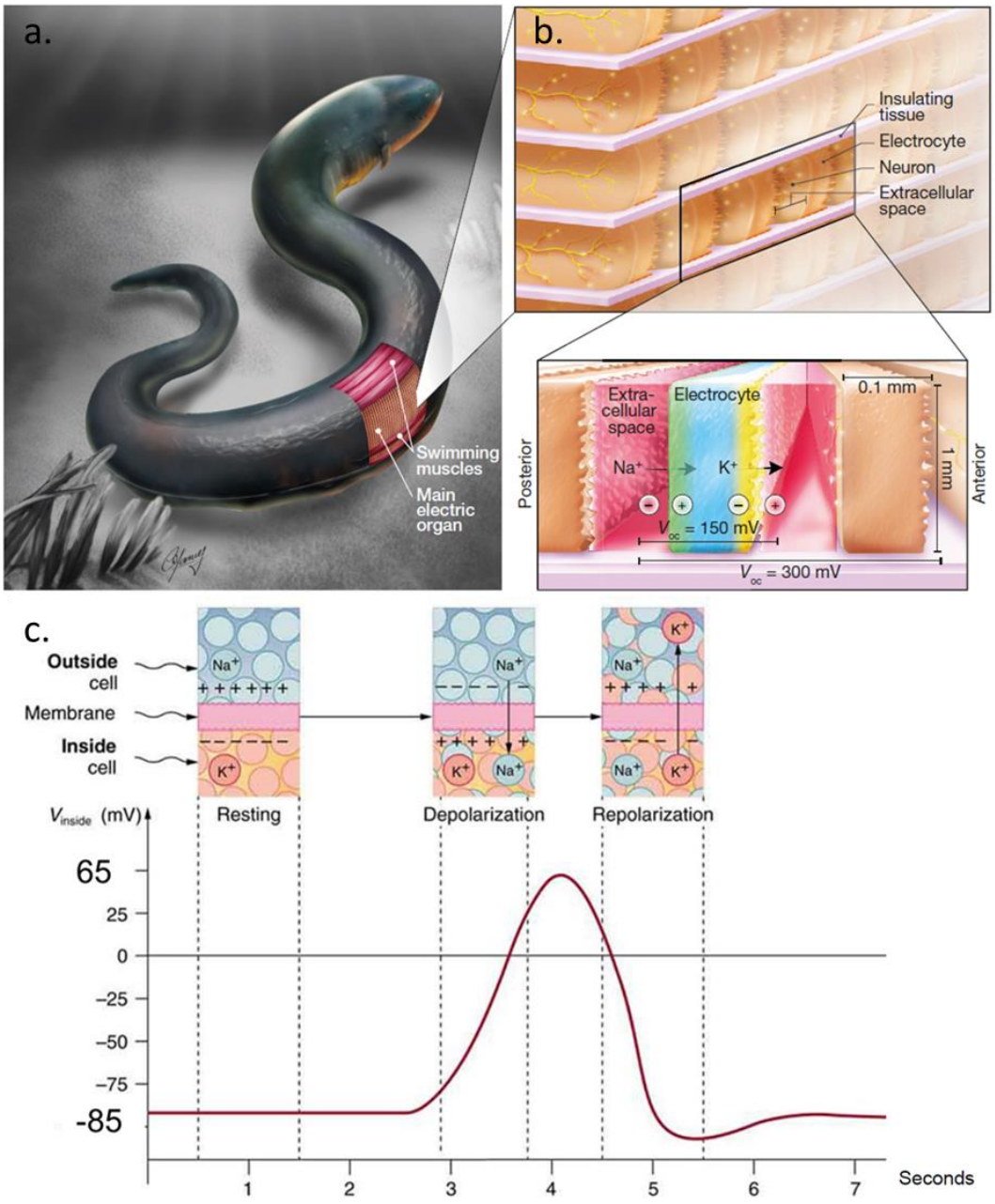

Figure 5 a. Morphology of an electric eel b. Arrangements of stacked electrocytes and electrocyte structure (Picture adopted from 8 with permission) [8] c. Mechanism of action of voltage generation by depolarization and repolarization(Picture adopted with permission from Animal Physiology Introductory by Sanja Hinic-Frlog-copyright 2019) [31]

A unique strategy that electric eel uses to generate electrical discharges has been developed at least six times in history for wide variety of usages such as bio-compatible batteries[32]. A novel electric eel inspired power concept is produced recently which can generate 110V at the open circuit as well as they are transparent, biocompatible, durable and not complicated to manufacture. Capability of such power generation from ion concentration gradient in excitable nano-cells that getting excited by sun irradiation could be a game-changing technology in future energy market.

To design a cell inspired by an electric eel, some major features including series setup of electrocytes, simultaneous excitation, and activation and enabling to regenerate large ion gradients are essential to achieve external electricity from internal excited cells. Mimicking these features is possible by using well-designed hydrogels.

2.4 Hydrogels

Hydrogels are a 3D network of polymer chains that are strongly connected together by cross-linkers and their hydrophilicity makes them the best choice for this project. Hydrogels with different ion concentrations and hydrogels with reverse ion selectivity can be combined to form an ionic gradient to generate power[33]. Fortunately, synthetic polymers usually have well-defined structures that can be modified to yield tailor able degradability and functionality. To form a hydrogel, water must be at least 10% of the total weight of the molecule. Several hydrophilic groups consist in hydrogel molecule chains[34].

There are different methods to classify hydrogels. Fig. 6 shows one well-known type of classification of hydrogels. They are classified based on the hydrogel's source, ionic charge, cross linker, preparation method, and stimuli responsive. To design an artificial eel, conductive

hydrogels must be used since the ionic conductivity is the vital key of having an ionic energy pathway.

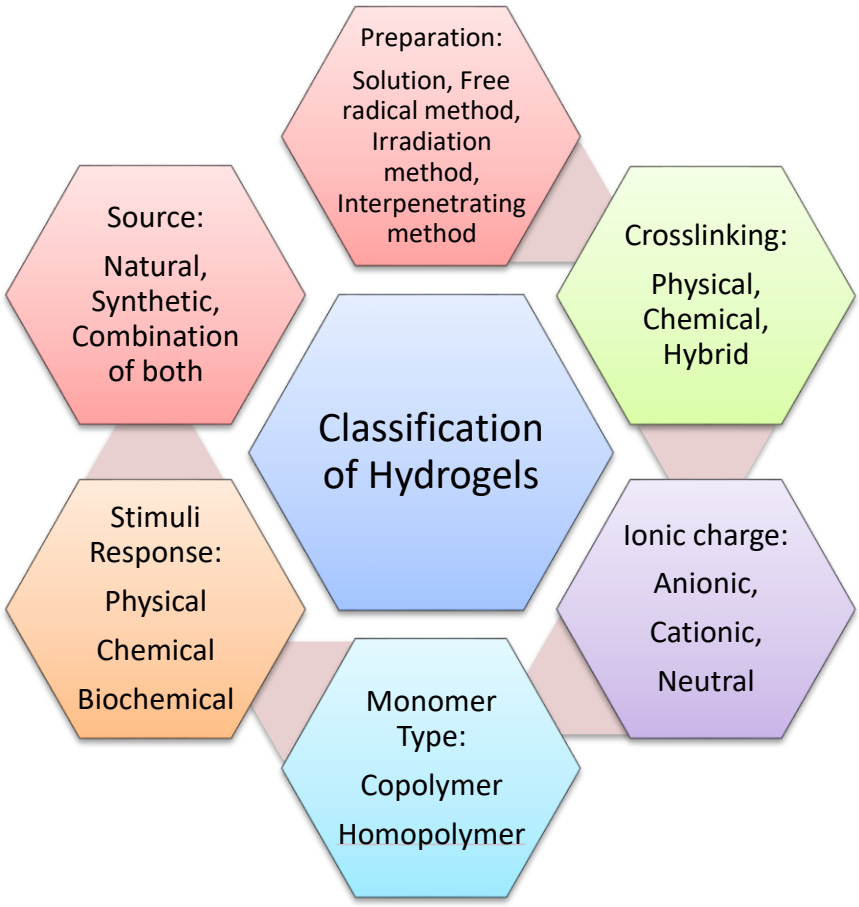

Figure 6. Different classification of hydrogels

2.4.1 Conductive Hydrogels

Conductive hydrogels (CH) consist of electron-conductive hydrogels, ion- conductive hydrogels, and a combination of electron and ion-conductive hydrogels [36]. The first group can be categorized in several ways however, one well-known classification contains single network electron-conductive hydrogels and double networks electron-conductive hydrogels which showed

higher mechanical stability, appropriate elasticity, and low surface friction which is very important in some bioelectronics such as bio-sensors [37]. Single network electron-conductive hydrogels including metal nanomaterial-based electron-conductive hydrogels, carbon material-based electron-conductive hydrogels, conducting polymer-based electron-conductive hydrogels, and electron- conductive hydrogels with hybrid conducting materials. On the other hand, ion-conductive hydrogels were introduced by the free movement of water molecules across the network of the polymers in hydrogels. Some materials have the ability to create free ions in water consists of acids like HCL, metallic salts (eg, NaCl/Na2SO4, KCl, LiCl, LiClO4, FeCl3/FeNO3, CaCO3/CaCl2, TbCl3, AlCl3), and ionic liquids) [25]. The benefits of using ionic-CH instead of electron-CH are reaching full transparency by ionic-conductive hydrogels as well as the ability to create electron double layers with different levels of electrons surfaces. This feature makes the ion- conductive hydrogels be able to act as an electrolyte in batteries or actuators. Moreover, they showed water retention capability and anti-freezing property which make them more durable and adaptable in the environment [26]. Fig. 7 shows the different applications of conductive hydrogels.

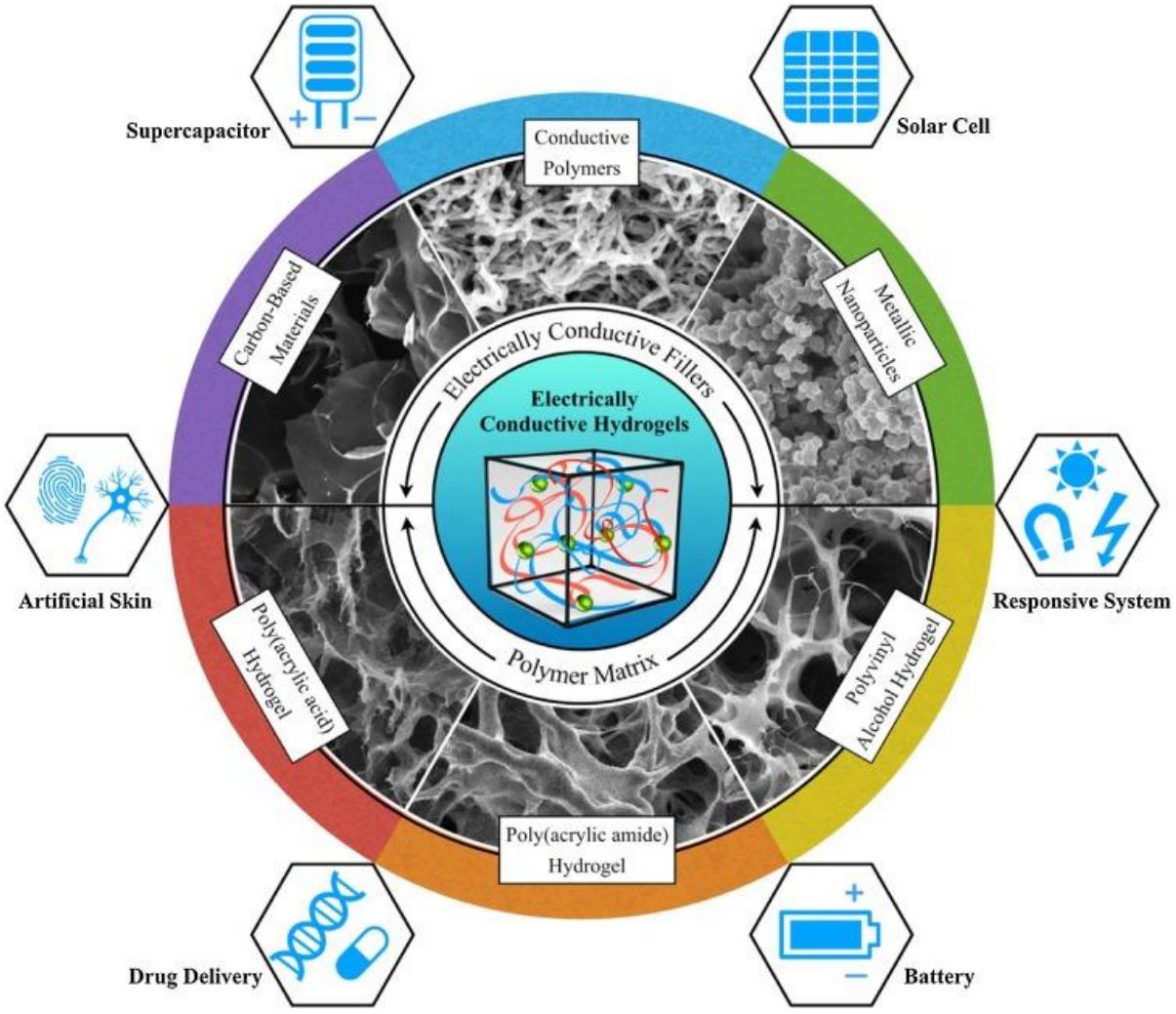

Figure 7 Application of conductive hydrogels(Picture adopted from 38 with permission) [38]

2.4.2 Polyacrylamide

Polyacrylamide is chosen in this work to mimic artificial electrocyte. In the literature, polyacrylamide based hydrogels showed great potential to serve as a conductive hydrogel in different technologies with different functions including sensors in metal nanomaterial-based electron conductive hydrogels, capacitors, energy storage, and conversion devices [33]. Polyacrylamide hydrogels (PAM) are made from free radical polymerization from acrylamide

monomers through cross-linking N, N'-methylene-bis-acrylamide, forming a soft gel. Polyacrylamide hydrogels are usually very stable and strong. Polyacrylamide hydrogels have sharp pH-volume transitions. As well, they have the ability to absorb water while the stretched polymer networks are able to limit osmotic swelling. Moreover, some challenges have been solved in polyacrylamide hydrogels such as water evaporation of conductive hydrogels by encapsulating the polyacrylamide hydrogels, and increasing the water retention capacity by introducing PAM-LiCl hydrogel which can act multifunctional as both light-absorber and transport layer in the hydrogel-based solar cells [39]. Here, we are merging the ionic-conductive polyacrylamide hydrogels with an artificial eel mechanism of action to produce electric shocks and utilize this strategy in sunlight energy conversion and storage technology.

2.4.3 Synthesis of hydrogels

Hydrogels are polymer networks that contain hydrophilic groups. Hydrogels are generally generated from hydrophilic monomers. They can be synthesized from synthetic or natural monomers [40]. The polymer chains must be cross-linked to form a hydrogel. Different types of crosslinkers have been used in literature. Crosslinking also refers to copolymerization with free radicals [41]. Crosslinking occurs by chemical reaction, physical interaction, and ionizing radiation. So, the three main compartments of synthesis of hydrogels are monomer, crosslinker, and initiator. Bulk polymerization, solution polymerization/cross-linking, Suspension polymerization, or inverse-suspension polymerization are the mainly used techniques in hydrogel synthesis [7]. Acrylamide-based hydrogels are usually polymerized by reverse suspension technique or dilute solution [35]. The solution polymerization has been used in this experiment. The polymerization initiates by solving the crosslinker and monomers at an appropriate

temperature and follows with UV-irradiation of the photoinitiator. The typical solvent used to synthesize PAM hydrogels is water. This technique is completely cost-efficient and non-complex without the need for high-temperature facilities.

Chapter 3

Materials and Methods

3.1 Artificial Electrocyte

3.1.1 . Artificial Electrocyte Design Principles

Engagements of thousands of electric organs in an electric eel in series and parallel, enable an eel to generate about 600 V [8]. To create an artificial electric eel current generator organ, the anatomy of the electrocyte has been mimicked. As was explained in section 2. 2, each electrocyte contains a posterior membrane and interior membrane which are bounded with connective tissues. There are several selective ion channels with selectivity to potassium ions and sodium ions. The transcellular potential is different across the membrane and the goal is to mimic these selective ion channels through the membrane by designed hydrogels. Fig. 8 shows the designed artificial electrocyte structure in comparison to the actual artificial electrocyte.

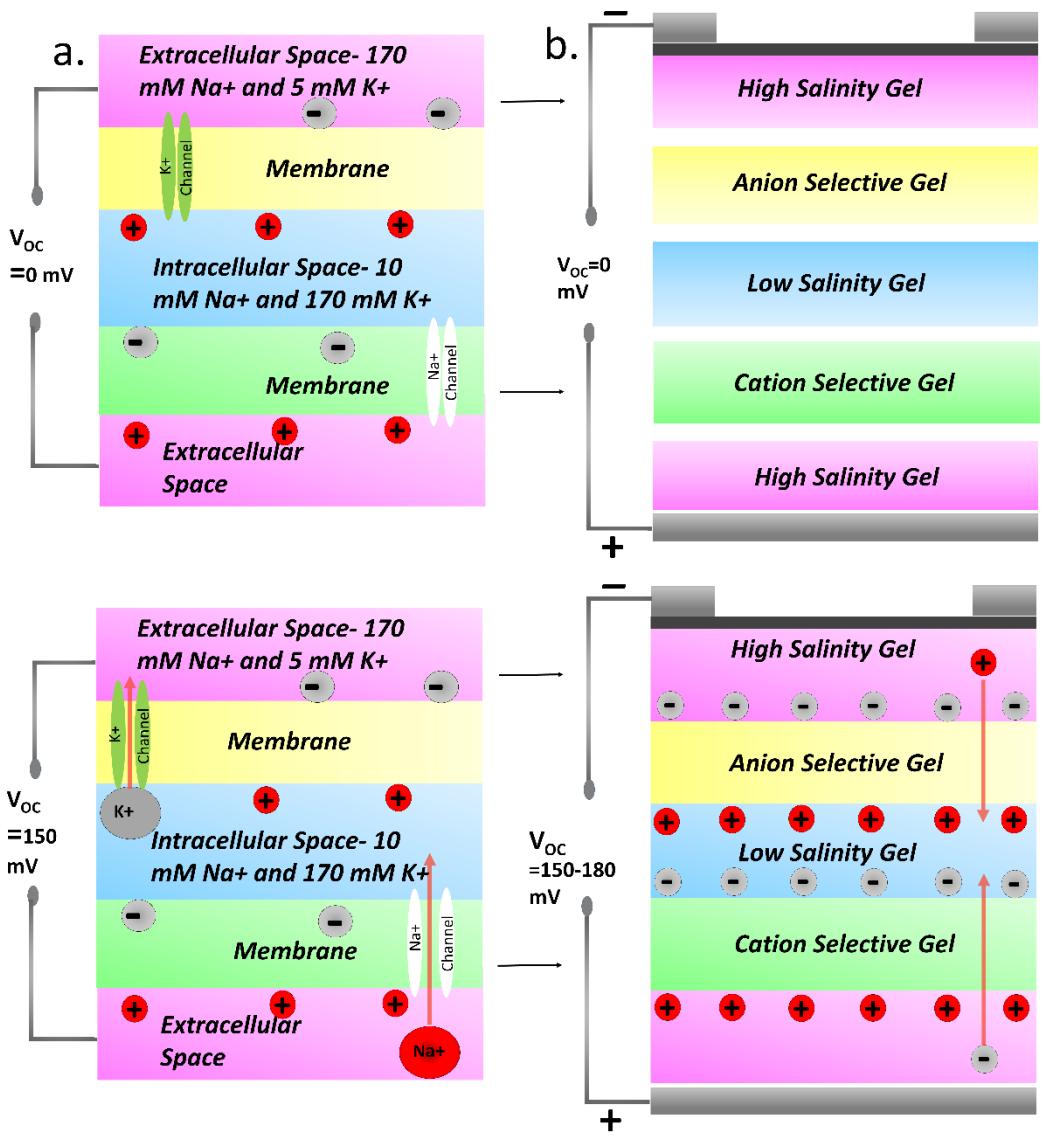

Figure 8 a. Mechanism of voltage generation in an actual electrocyte. b. Mechanism of voltage generation in an artificial electrocyte

The designed structure of the artificial electrocyte contains two polyacrylamide hydrogels with different concentrations of sodium and chloride ions called high salinity hydrogel and low salinity hydrogel. High salinity and low salinity hydrogels play the extracellular and intracellular space's

role respectively. Mimicking the posterior and interior membrane has been done by using cationic and anionic hydrogels. Cation selective and anion hydrogels act as a membrane with selective ion channels however, the artificial membranes are only able to separate positive and negative ions. This tetrameric hydrogel sequence is able to generate an ionic conductive energy pathway by utilizing ionic gradient electromotive force.

The hydrogel's amazing properties such as free movement of ions between polymer chains, straightforward synthesis process, biocompatibility, and low manufacturing costs make it a proper material to mimic the electrocyte organ. Fig. 9 shows the design of the fluidic printed artificial electrocyte. By contacting the gel cells, the ion concentration gradient causes a flow of free ions across the cell due to the osmotic effect. The cations move toward cation-selective gel and anions move toward anion-selective gel. As a result, two sides of low salinity gel have different polarity in turn, different transcellular potential.

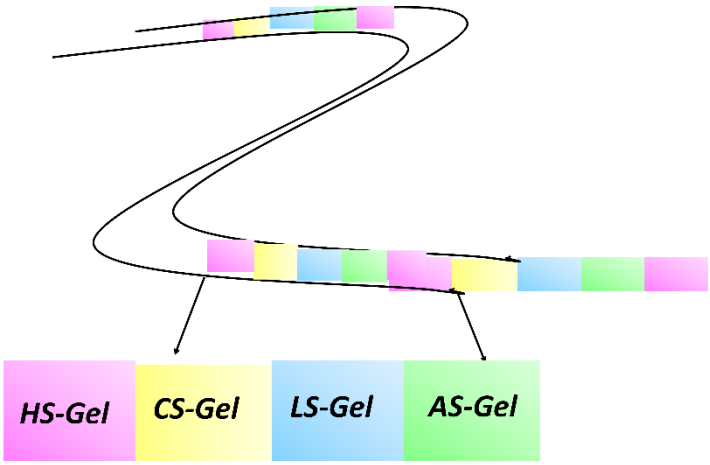

Figure 9 Schematic view of the fluidic printed artificial electrocyte, a sequence of high salinity (HS) gel, cation selective (CS) gel, low salinity (LS) gel, and anion selective (AS) gel. Then the pattern repeats starting with a high salinity gel.

3.1.2 Synthesis and Fabrication Process

At first, the polyacrylamide hydrogel with different components have been synthesized. For fluidic organ containing aqueous plugs, the gel solutions contain characteristics of: low-salinity gel: acrylamide, 2-hydroxy-4'-(2-hydroxyethoxy)-2-methylpropiophenone (henceforth photoinitiator), and 37.5:1 acrylamide/N,N′-methylenebisacrylamide. High-salinity gel: acrylamide, 2-hydroxy-4'-(2-hydroxyethoxy)-2-methylpropiophenone (henceforth photoinitiator) and 37.5:1 acrylamide/N,N′-methylenebisacrylamide. Cation-selective gel: 2-Acrylamido-2-methylpropane sulfonic acid, 2-hydroxy-4'-(2-hydroxyethoxy)-2-methylpropiophenone (henceforth photoinitiator) and 37.5:1 acrylamide/N,N′-methylenebisacrylamide. Anion-selective gel: (3-Acrylamidopropyl)trimethylammonium chloride, acrylamide, and 37.5:1 acrylamide/N,N′-methylenebisacrylamide. We used the solution based method in order to synthesis the hydrogels. To prepare the PAM hydrogels, the pre gel solution was created by using a photo-initiated polymerization process. 2-hydroxy-4'-(2-hydroxyethoxy)-2-methylpropiophenone was the photoinitiator. The photoinitiator and aforementioned salts have been added to the acrylamide/N,N′-methylenebisacrylamide solution and the polymerization took place for 5 hours at 25˚ Celsius.

To create the fluidic printed artificial electrocyte, the sequence of the four type PAM hydrogels were injected in a polyester transparent tube with thickness of 0.2 mm. Then, we cured the gels under "UVP 302nm Analytik-Jena", at 10 cm distance, and for 90 seconds. These gels are pushed together. The high/low-salinity gels are produced separately and stacked on the other gels by applying light pressure.

For surface dot printed hydrogels on substrate, the gel solution characteristics include: low-salinity gel containing acrylamide, glycerol, 2-hydroxy-4’-(2-hydroxyethoxy)-2-methylpropiophenone (henceforth photoinitiator) and 37.5:1 acrylamide/N,N′-methylenebisacrylamide. High-salinity gel: acrylamide, 2-hydroxy-4’-(2-hydroxyethoxy)-2-methylpropiophenone (henceforth photoinitiator) and 37.5:1 acrylamide/N,N′-methylenebisacrylamide. Cation-selective gel: -Acrylamido-2-methylpropane sulfonic acid, 2-hydroxy-4’-(2-hydroxyethoxy)-2-methylpropiophenone (henceforth photoinitiator) and 37.5:1 acrylamide/N,N′-methylenebisacrylamide. Anion-selective gel: (3-Acrylamidopropyl)trimethylammonium chloride, acrylamide, and 37.5:1 acrylamide/N,N′-methylenebisacrylamide. The high/low-salinity gel solutions are printed onto a flat polyester substrate without any geometrical pattern. As well, the cation/anion-selective gels are printed onto the same substrate. Then the gels cured for 10 seconds at 10 cm distance with “UVP 302nm Analytik-Jena”. After curing, two substrate were connected together to make a conductive ionic way between the hydrogel drops.

3.1.3 Measurements

All voltage, current, and resistance measurements have been done using a Keithley DMM6500 multimeter at 25˚Celcius. Aluminum wires were used at the two ends of each artificial organ and the wires are cured in the high salinity hydrogels at the two ends. To measure the properties of the cells, the tubes get stacked in parallel. Fig. 10 shows the synthesized hydrogels, the structure of one fluidic printed tetrameric cell, two fluidic printed cells in series, and the arrangement of 6 stacked cells in parallel which each tube contains three tetrameric cells, and finally, the voltage measurement process.

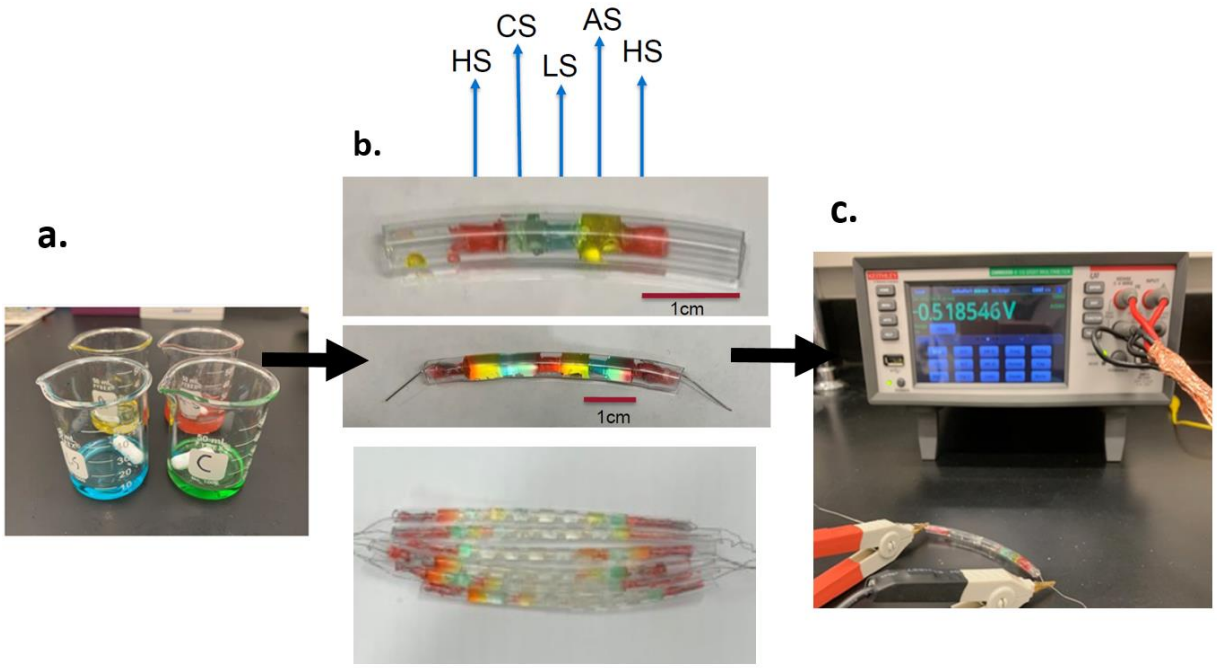

Figure 10 a. synthesized hydrogels, b. structure of one fluidic printed tetrameric cell, two fluidic printed cells in series, and an arrangement of 6 stacked cells in parallel in which each tube contains three tetrameric cells, and c. the voltage measurement process.

3.2 Electric Eel Inspired Solar Cell

3.2.1 Design Principles

To mimic the electrocyte mechanism of action and merge it with solar cells functionality, proper light absorption property, efficient ionic charge transport, and free charges collection should be implemented [7]. First of all, the light absorption property of electric eel-inspired solar cell must be reliable enough to generate photocurrent. The ionic electromotive force caused by ion concentration is a key factor to transfer the free ionic charge carriers and, finally, the collection of free charges should be optimized by cation and anion transfer layer.

Natural dyes are aimed to integrate with stacked hydrogel-based structures inspired by the artificial eel. The interface and recombination sites will be different and highly depends on how the energy transfers from photo-induced electron/hole pair to various ions in the hydrogel structure. My results indicate that energy transfer from electron-hole pair generation in black hydrogel using graphene to Na and K ions is a possible and favorable process in stacked hydrogels. Fig. 11 shows the structure of my first-generation electric eel-inspired solar cell. The proposed device is based on stacking an upper metallic contact, a low-salinity hydrogel, a cation-selective hydrogel, a high-salinity hydrogel, an anion-selective hydrogel, and a second low-salinity hydrogel ended by the metallic contact. This device is inspired by its solid-state counterpart of stacked semiconductor pin junctions to form a PV device. Upon solar radiation absorption, an ionic conductive pathway is formed due to an ionic gradient that results in an open-circuit voltage. The most important challenges in the proposed device are to increase the efficiency of light absorption and trapping in the device and mitigating the ion/charge trapping/recombination in various interfaces. Note that trapping and recombination of cation/anion are less probable than trapping and recombination of electron/hole in semiconductors [21].

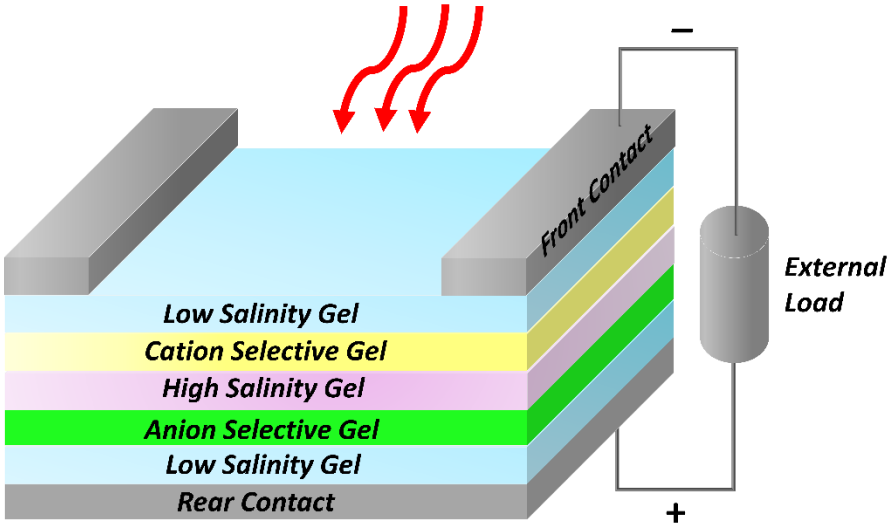

Figure 11 Schematic of the electric-eel inspired hydrogel solar cell.

3.2.2 Synthesis and Fabrication Process

The synthesis process and the components of each gel are completely the same as the synthesis process of the dot printed artificial electrocyte (section 3.1.2). The solar cells have been fabricated by applying each gel on top of the cured layer. The UV lamp used for this project is aUVP 302nm Analytik-Jena. The curing of each layer was 20 seconds. All printed solar cells have a two centimeters diameter and different thicknesses of layers have been investigated.

3.2.3 Measurements

At first step, the light absorption of each gel has been investigated by recording the UV-Vis spectrum. All absorptions have been recorded by UV-2501PC by Shimadzu. The effects of dyes, thickness, and type of gels have been reported in the results part. Secondly, photoconductivity of each layer as well as arrangements of low/high salinity gels, low/high/low salinity gels, and 5 layers gels have been captured. All photoconductivity measurements have been done using a JH-

Technologies Inc, instrument under white light. Then, the I-V characteristics of all printed solar cells were recorded. At first, the 5 layers cell including low salinity, cation-selective, high salinity, anion-selective, low salinity layers fabricated. To improve the efficiency of the solar cell, three layers containing low/high/low salinity gels has been fabricated. All solar simulator measurements were done using a Solar Simulator 1000-Optical Radiation Corporation device at air mass 1.5 and standard conditions of 100 mW/cm^2 for 15 seconds. Fig. 12 shows a solar cell sample and measurement process.

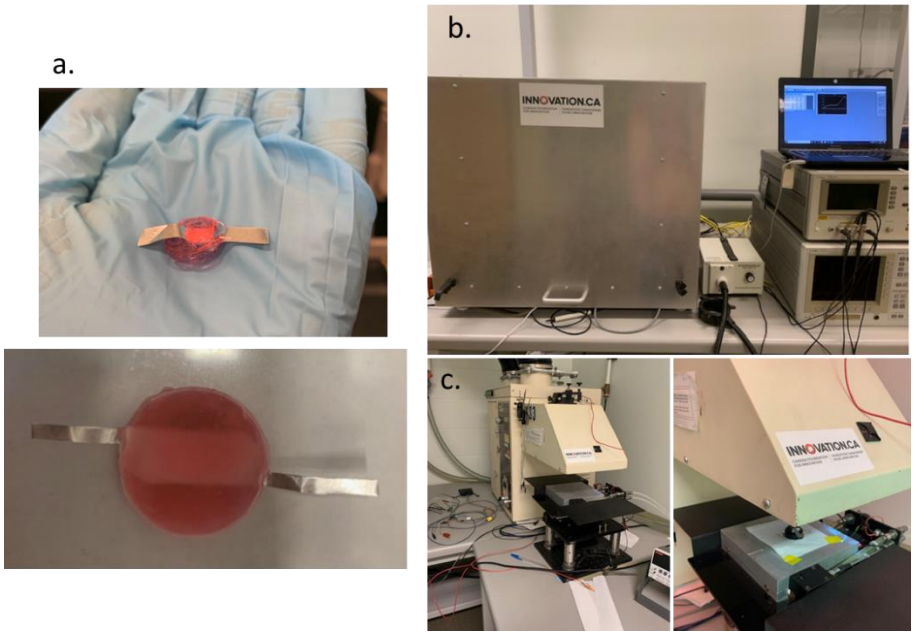

Figure 12 a. Electric eel-inspired ionotronic solar cell b. Photoconductivity test, and c. solar simulator test process.

3.3 Materials

We purchased (3-Acrylamidopropyl)trimethylammonium, 3-Sulfoporpyl acrylate potassium salt, 2-Acrylamido-2-methylpropane sulfonic acid and 2-hydroxy-4'-2(2-hydroxyethoxy)-2-methylpropiophenone (henceforth photoinitiator) all from Sigma-Aldrich. As well we purchased

from Bio-Rad, 37.5:1 acrylamide/N,N′-methylenebisacrylamide in 40% mix solution in water. The P100 hydrophilic solution was purchased from Joninn. A4-sized uncoated polyester overhead transparencies with a thickness of 0.1mm was purchased from Avery.

Chapter 4

Results and Discussion

Nowadays, bionics attracted great interest during the last decade and bioelectricity is an important trend in technology. Also, no one can deny that the fascinating mechanism of generating external discharges from excitable cells in electric eel has a huge potential to inspire researchers to design and develop electrochemical devices using the same principles. Having these concepts in mind, theoretically, it is possible to use ionic gradient driving force to develop a light-harvesting device. In this regard, we will investigate the practicality of creating an artificial electrocyte with hydrogels, its conductivity, and its durability (section 4.1). In the next step, the optimized design is utilized to fabricate an electric eel-inspired solar cell (section 4.2). The light-harvesting properties of the designed cell have been investigated. The eel-inspired solar cell is then characterized and enhanced by changing its design structure.

4.1 Artificial Electrocyte

To generate the artificial electrocyte capable of creating a potential difference in open circuit, 4 types of polyacrylamide based hydrogels including high salinity/low salinity hydrogels as extracellular space/intracellular space and cation-selective/anion-selective hydrogels as the semi-permeable membrane are designed. Different ion concentrations due to negatively/positively charged monomers synthesized hydrogels mimic the asymmetric transmembrane potential between innervated and non-innervated membranes. Different types of hydrogel have to be synthesized in order to mimic the nano-conductors of electrocyte membrane such as ion channels

and pumps which act selectively to let N^+/K^+ go through them to make the cell depolarized/repolarized.

4.1.1 Surface Printed Artificial Electrocyte

At first, a surface printing method was conducted to investigate the ability of hydrogels to create a voltage difference via electrocyte principle. Fig. 13 shows a surface-printed cell, three cells in series and two cells in series before and after connection. Each tetrameric gel cell consists of a sequence of high salinity, cation-selective, low salinity, and an onion selective gel with an ending of a high salinity gel. The sequence of gels has been connected by a narrow needle to create an ionic pathway in order to capture the different potentials between high salinity gels at the two ends. Fig. 14 shows the open circuit voltages of a gel cell as a function of the volume of each gel. Charge carriers increase by increasing the volume of the gel leads to getting higher voltage difference however, the relationship is not linear since in high concentration of ions the recombination rate enhances. In other words, the conductivity reduces as a result of higher contractions between the charges carriers since the mean distance between the ions decreased. Also, open circuit voltage increase by increasing the volume of the gels. Different ion concentration provides a condition in which an electromotive force is created across the tetrameric gel-cells. By stacking the gel-cells in series, the different potentials across the sequence of gels will be added up (see Fig. 15).

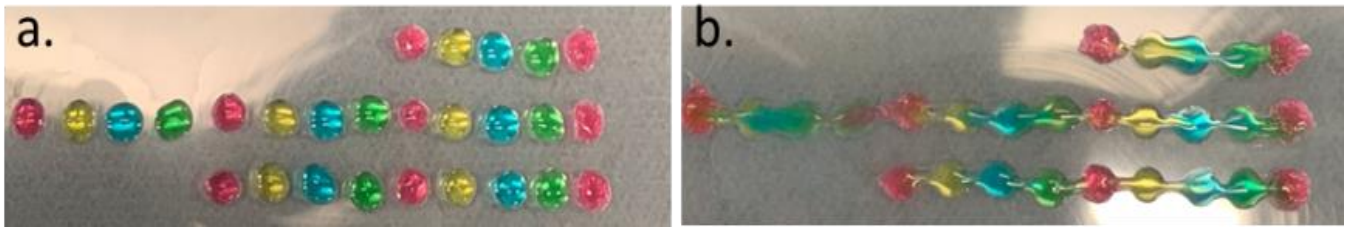

Figure 13 Surface printed gel cells a. before and, b. after connection

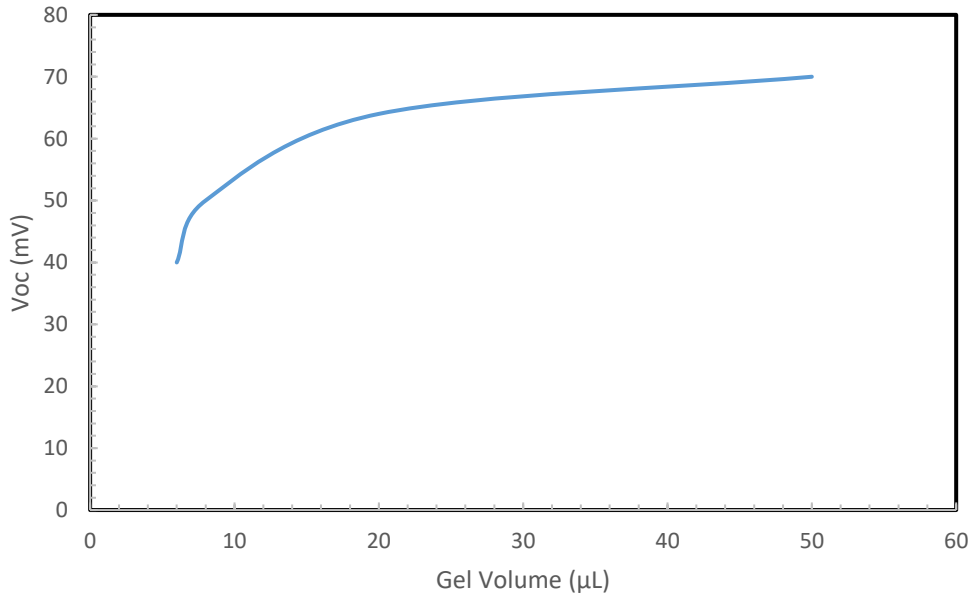

Figure 14 Open circuit voltage of artificial electrocyte as a function of gel volume

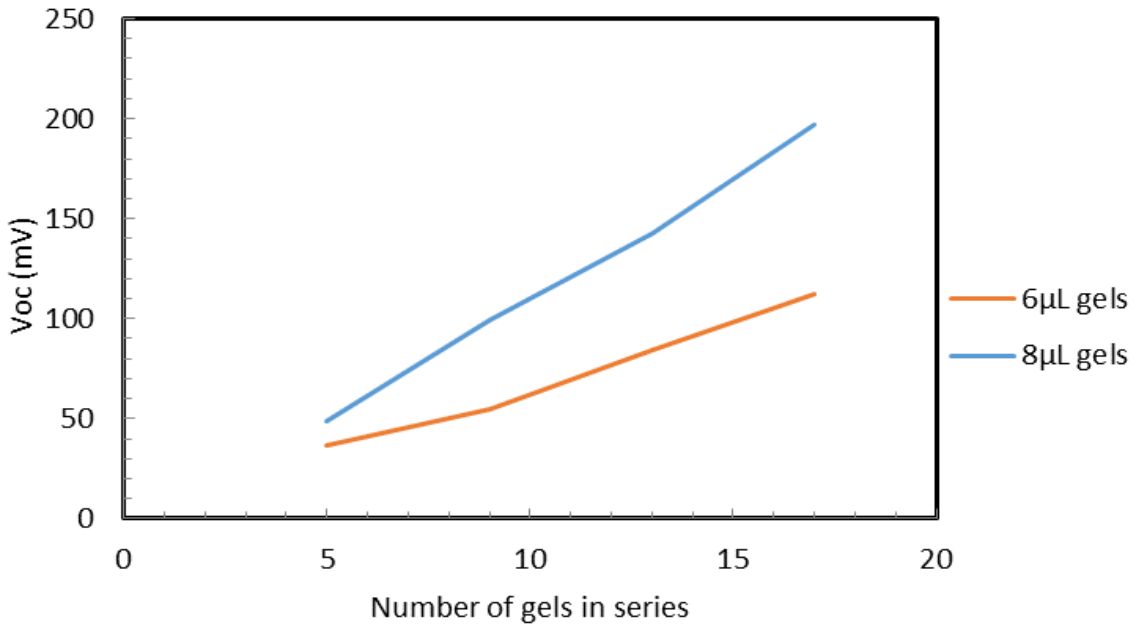

Figure 15 Open circuit voltage of artificial electrocyte as a function of numbers of gels

To improve this gel-cells utilization in an actual synchronous artificial electrocyte and after optimizing the hydrogel synthesis process, an improved assembly strategy has been used. Fig.16 displays the surface printed artificial electrocyte established by mechanical contact of two complimentary gel patterns. The sequence of three gel-cells in series reached approximately 75 mV after the connection of 8µL hydrogel lenses. The generated electrical potential difference in this artificial organ is limited. The curing process toughens and solidifies the gels by creating a tridimensional polymer network, in turn, polymer chains in the 3D network have more interaction. Also, the water of the gel which makes the hydrogel an ionic conductor, evaporates easily during the curing process therefore, the cured hydrogel shows less conductivity in comparison with gel cells. One challenge in this strategy is that the conductive ionic pathway is too small and the

thickness of the lenses is an order of magnitude larger than the actual electrocyte (approximately 100 µm). It is possible to minimize the resistance by printing the lenses on a patterned substrate.

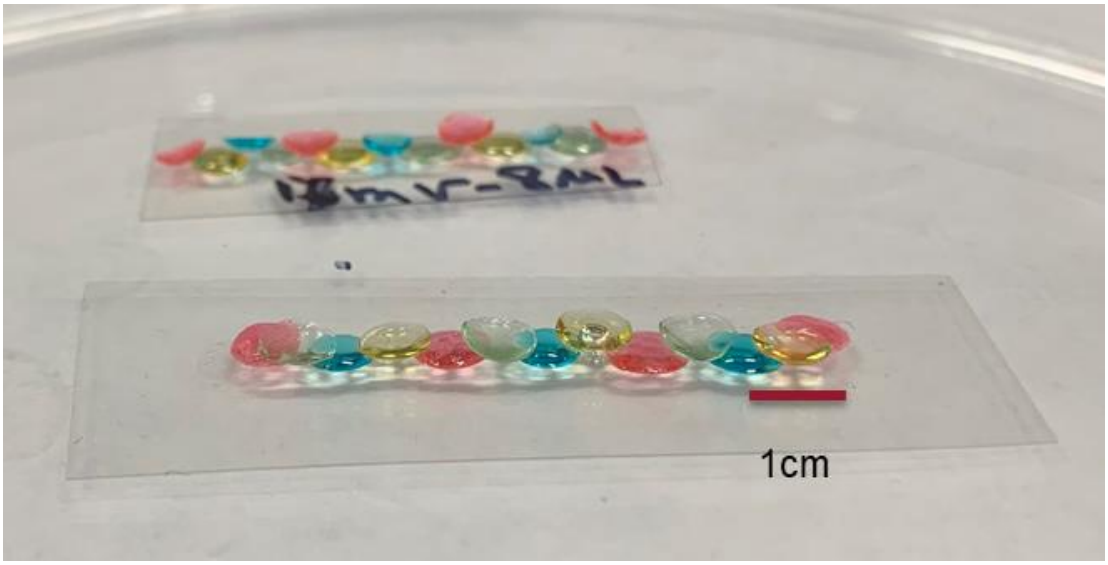

Figure 16 Surface printed artificial electrocyte after curing and connection

4.1.2 Fluidic Printed Artificial Electrocyte

To improve the performance of the artificial electrocyte, a fluidic printing strategy has been implemented. Each tetrameric cell consists of four types of hydrogels including high salinity, cation-selective, low salinity, and anion-selective hydrogels with a high salinity hydrogel at the end of the cell. In this strategy, a series of gels are positioned sequentially. Highly concentrated and low salinity areas express the extracellular and intracellular area with the ability of electrical potential generation across the entire artificial organ with fluidic ion-gradient force. To optimize the hydrogels synthesis process, at first the proper curing time has been investigated. Fig.17 indicates that by increasing the curing time, the electrical potential difference drops down. In semi-

fluidic conductive materials, the mobility of charge carriers are completely dependent on the ion concentration in higher concentrations, which in turn, by evaporation of water molecules and formation of a third polymer network, the mobility drops down. Not enough 3D networks have been formed for a curing duration of less than 90 seconds.

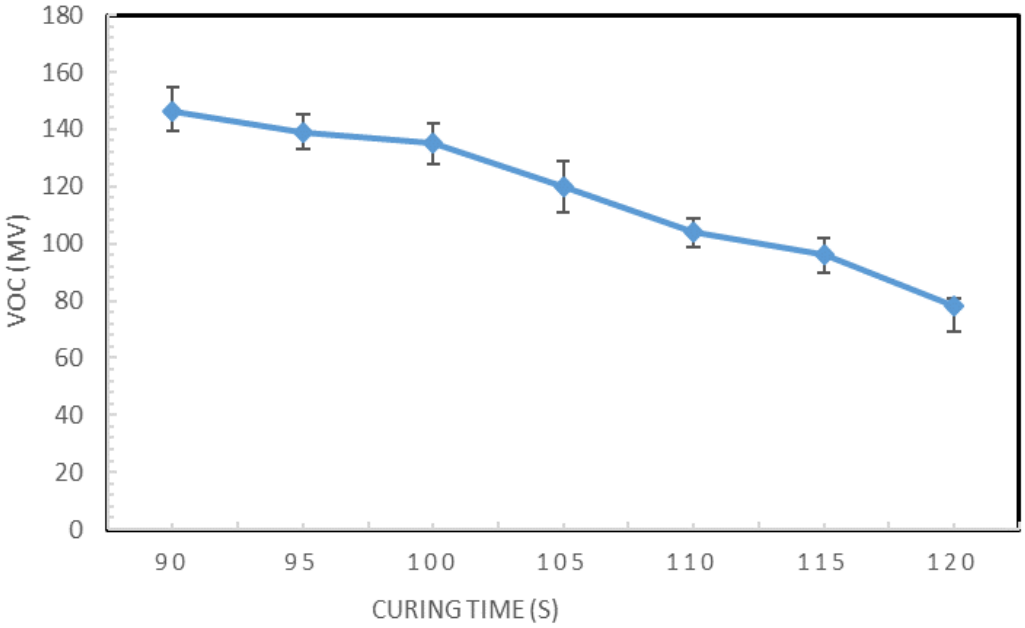

Figure 17 Open circuit voltage of fluidic printed artificial electrocyte as a function of curing time of gels

In the next step, the electrical potential difference and current of an artificial electrocyte consisting of one cell have been investigated. Artificial electrocytes with different volumes of gels showed different results. The thickness of gels plays an important role in the electrical properties of the artificial electrocyte. Fig. 18 displays the short circuit current as a function of the gel volume. The highest short circuit current was obtained from the artificial organ with a gel volume of 10 µL. A sequence of five 10 µL gels with a total thickness of 6.519×10^{-3} m reached approximately 2.5 µA while the cell with 100 µA gels with a total thickness of 6.519×10^{-2} m showed about 1 µA.

Lower thickness results in higher conductivity due to the proportional relationship of the internal resistance and the thickness of gels. Moreover, by increasing the thickness of each gel, interactions between positive and negative ions inside of each gel increases, in turn, the ion-pairs recombination rate is higher, and capturing the ions before recombination is a challenge in thicker gels.

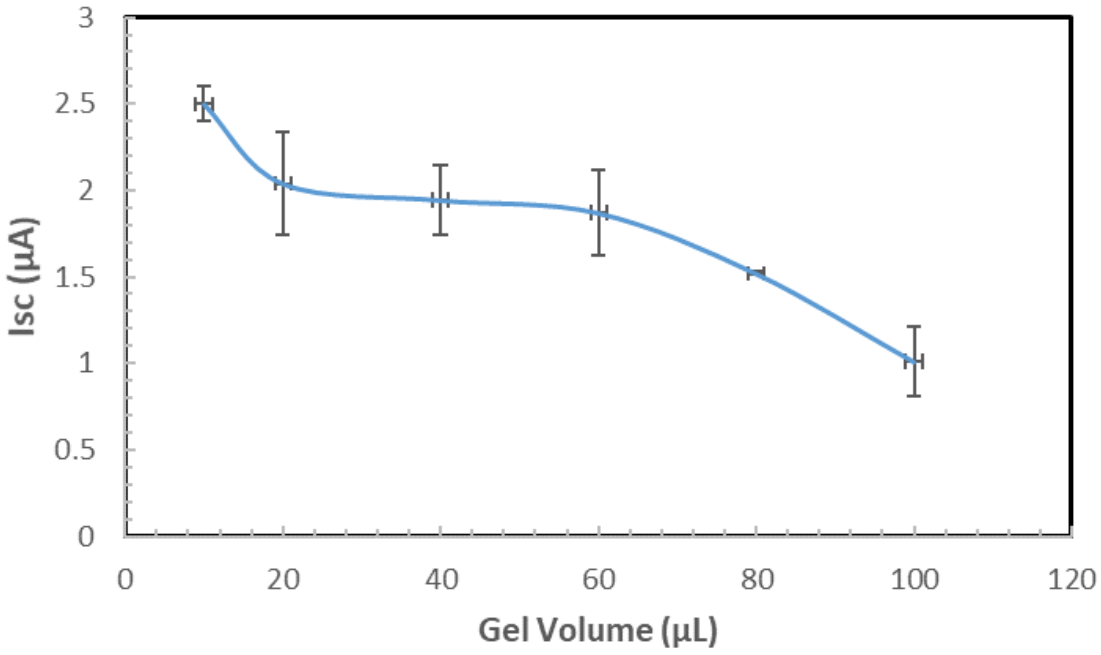

Figure 18 Short circuit current of the fluidic printed artificial electrocyte as a function of gel volume

Fig. 19 shows the open-circuit voltage of the artificial electrocyte as a function of volumes of each gel. The plot indicates that the higher the volume of the gel, the higher the electrical potential difference between high salinity gels at the two ends. The concentration of charge carriers is ten times higher in 100 µL gels than 10 µL gels which means the total potential energy of the former gel should be higher.

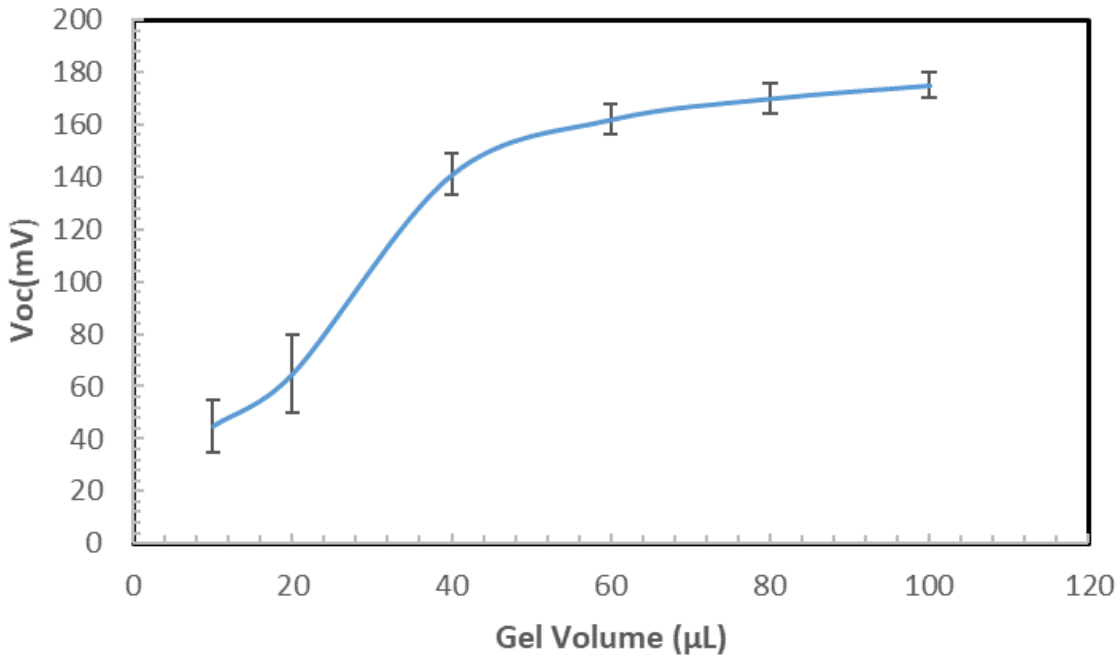

Figure 19 Open circuit voltage of the fluidic printed artificial electrocyte as a function of gel volume

To determine the contribution of different gels in the whole cell, the resistance of each individual gel as well as a complete cell has been obtained (Table.1). A whole cell containing five hydrogels showed approximately 0.318 Ωm^2 resistance per area. In addition, the low salinity gel resistance obtained by direct DC measurements and is about 0.176 Ωm^2 however, the resistance of cation-selective and anion-selective gels is less than 50% of the resistance of the low salinity gel. These huge differences can be explained by the compartments of each gel. For example, 2-acrylamido-2-methylpropane sulfonic acid and (3-Acrylamidopropyl)-tri methyl-ammonium are the main components of the cation-selective gel and anion-selective gel which makes them ionic gels with several ions bounded to the polymer chain. The mobile ions contribute to conductivity by forming a dual conductive network. On the other hand, the high salinity gel showed resistance of less than 0.003 Ωm^2 due to a high concentration of mobile Na+ and Cl- mobile ions in it.

Table 1. Estimated resistance of the hydrogels of the artificial electrocyte

Gel	Full Cell	Low Salinity Gel	Cation Selective Gel	Anion Selective Gel	High Salinity Gel
Area normalized Resistance (Ω/m^2)	0.318	0.176	0.085	0.056	0.003

Comparison of characteristics between my fluidic artificial electrocyte and an actual electrocyte is provided in Table.2. By comparing the design of the presented artificial electrocyte with an actual electrocyte, the performance improvement can be predicted for the future. One of the critical challenges is the comparably high thickness of the gels. For instance, the thickness of an electric organ in an electric eel is about 1.1×10^{-4} m, while in our model the thickness of 40 µL gel cells is approximately 2.607×10^{-2} m. In this condition, the absolute ion permeability of the gels is 10 times smaller than the actual cell membranes in an electrocyte. The internal resistance of the low salinity gel as a function of the thickness of the gel is shown in Fig.20. As it is expected, reducing the thickness of the gels leads to a decrease in internal resistance. One strategy to improve this drawback is printing the gels in the shape of layers. In this strategy not only the thickness of the cell is reduced but also, the contact surface area is widened as which means the total resistance of a full cell will be reduced.

Table 2 Comparison of characteristics between fluidic artificial electrocyte and actual electrocyte

Source	Cross-Sectional Area of the Cell (m^2)	Thickness of the Cell (m)	Open Circuit Voltage (V)	Resistance per Area of the Cell (Ω/m^2)
Electrocyte of a Live Electric Eel[31]	3.4×10^{-3}	1.1×10^{-4}	0.16	4.82×10^{-4}
Fluidic Printed Artificial Electrocyte	7.7×10^{-6}	2.607×10^{-2}	0.15	3.18×10^{-1}

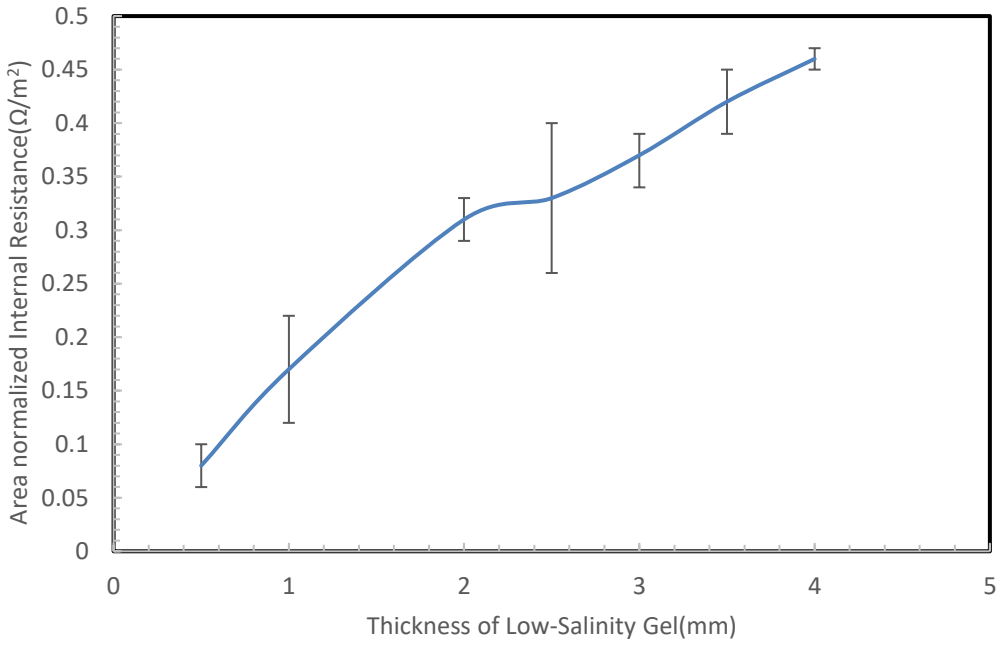

Figure 20 Internal resistance of gels as a function of thickness

4.1.3 Design Improvement for Electrical Property Enhancement

Fluidic assembly enables the formation of a parallel stacked artificial electrocyte. In other words, it makes it possible to generate stackable artificial electrocytes. Fig. 21 shows the open-circuit voltage characteristics of one cell, three tetrameric cells in series, and three stacked in a parallel set of three tetrameric cells. By placing tetrameric gel cells in series, open circuit voltage expands linearly. Voltage in the value of 1.27 V can be obtained by stacking 7 tetrameric gel cells in series (see Fig. 22).

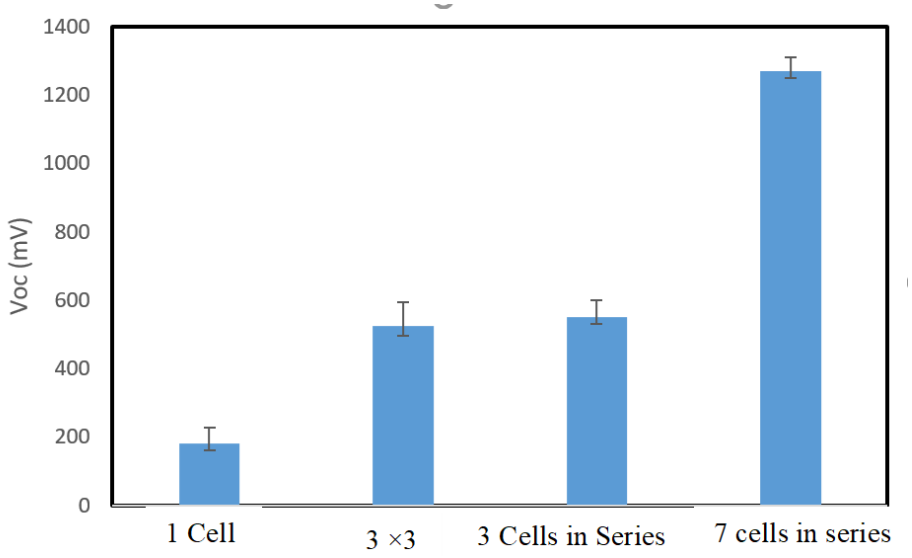

Figure 21 Open circuit voltage of the fluidic printed artificial electrocyte with different arrangements

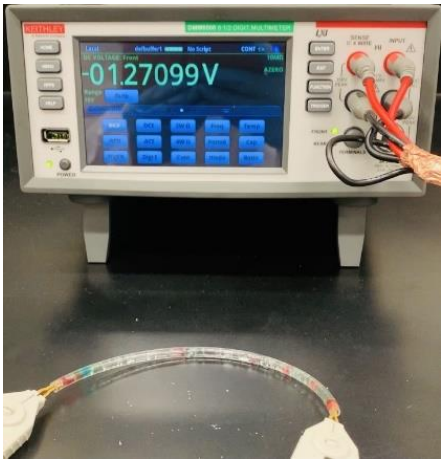

Figure 22 Open circuit voltage of 7 tetrameric fluidic printed cells

Fig.23 expresses the comparison of the short circuit current between different arrangements of the artificial electrocyte. When cells are added in parallel, the short circuit current increases. Stacked three rows of cells containing three series cells in each row obtained 6.4 µA, while the single cell showed about 2.5 µA.

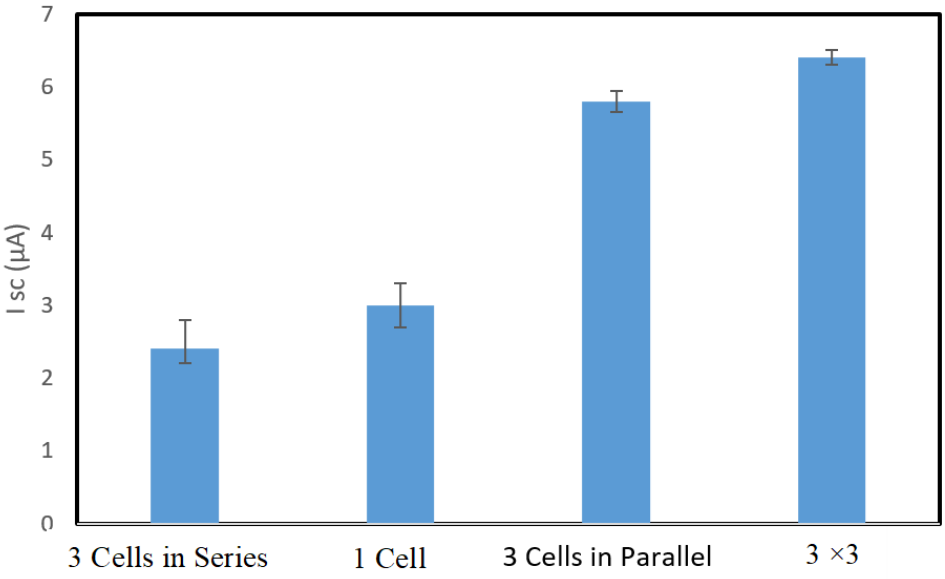

Figure 23 Short circuit current of the fluidic printed artificial electrocyte with different arrangements.

An important challenge in hydrogel-based soft matters is the difficulty of reaching long-term durability and stability. In order to improve the lifetime of this artificial electrocyte, the self-discharge of the cell has been captured as a function of time. The artificial electrocyte will completely discharge after 600 minutes, and after 270 minutes, the cell lost 45.6% of its charge. Hydrogels consist of more than 80% of water. The hydrogels naturally get dry in ambient air conditions. Water molecules play the main role in the conductivity of hydrogels. Evaporation of water in ambient air makes the hydrogel too viscous and its stiffness will drop the mobility of free ions between the polymer chains. Most hydrogel-based electronics suffer from a short conductivity lifetime of hydrogels. Encapsulation of the cell is one of the strategies that will enhance the durability of hydrogels. To overcome this drawback in fluidic printed artificial electrocyte, one cell has been encapsulated by polyester films. A comparison between the regular and capsulated cell is shown in Fig.24. The basic encapsulation improved the discharge rate by about 22.6 %.

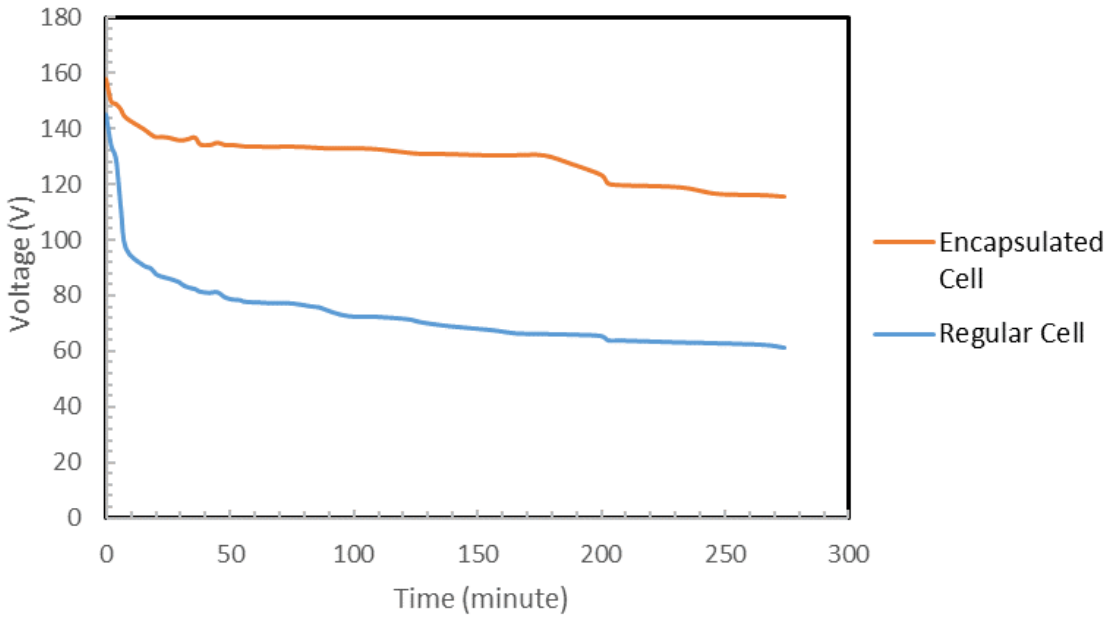

Figure 24 Open circuit voltage of fluidic printed artificial electrocyte as a function of time for a regular and encapsulated sample

4.2 Electric-Eel Inspired Solar Cell

Hydrogel-based ionotronic devices have already enabled the fabrication of compact and efficient batteries, supercapacitors, and fuel cells [18]. Hydrogel optoelectronic devices devised with varied combinations of optical transparency and electrical conductivity have been introduced for applications in luminescent and liquid crystal devices as well as for touchpads and sensors [18]. Inspired by the merits of dye-sensitized solar cells, electric eel mechanism of action, and conventional junction-based PV devices, the ionotronic photovoltaic solar cell is produced based on two distinct strategies: 1) the development of an ion-based p-n type multijunction PV cell and 2) a radically new cell, based upon the artificial eel [19]. Light harvesting property, photocurrent

generation potential, and solar energy conversion efficiency are presented in the following sections.

4.2.1 Light Absorption Properties

The main step in all types of solar cells is their ability to absorb sunlight. In this section, the light-harvesting property of each hydrogel is investigated. UV-Vis analysis was conducted to find the effect of thickness, type of gel, and the dyes used to improve the absorption property of the hydrogels. Fig. 25 displays the comparison of the absorption spectrum of high salinity gel for 1.5 mm, 3mm, and 6 mm gel thicknesses. The thickness of the active layer in solar cells always plays a vital role in light absorption since the absorption coefficient is dependent on the thickness of the layer. High salinity gel in the first generation of the electric eel-inspired solar cell represents the main active layer. Comparing the hydrogel without dye, the dyes improved the hydrogel absorbance. The maximum absorbance occurred around 534 nm for all the thicknesses with red dye, which is predictable. The 6 mm sample showed much higher absorbance than the 3 mm and 1.5 mm samples. The UV-Vis spectra display that by increasing the thickness of the gel, the absorbance will increase as well. However, in order to optimize the integration of light-harvesting ability with transfer and dissociation of the charge carriers, 1.5 mm of high salinity gel with dye provides the proper absorbance needed to generate charge carriers.

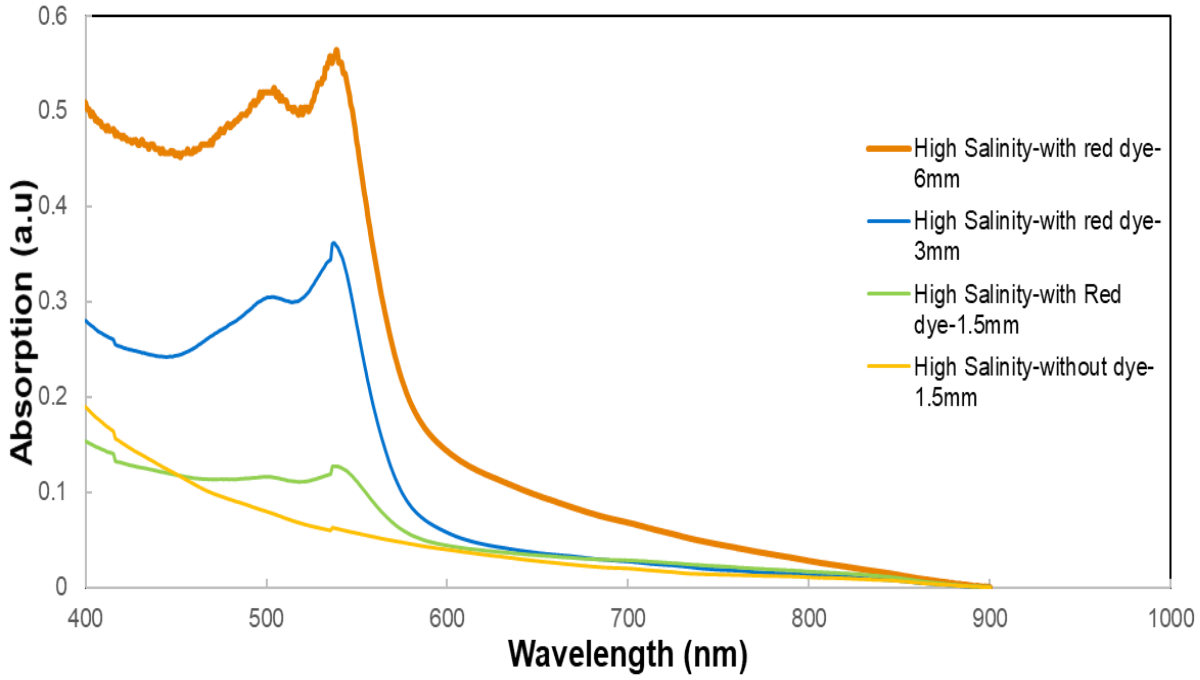

Figure 25 Absorption spectrum of high salinity gel for 1.5 mm, 3mm, and 6 mm gel thicknesses.

Further investigation was carried out to obtain information about the light absorption property of other synthesized hydrogels. Three layers of hydrogels with a thickness of 1.5 mm were prepared from the cation-selective gel, low salinity gel, and high salinity gel. Also, a comparison of the absorbance of these gels with a sample of PEDOT:PSS was conducted. Fig. 26 shows the UV-Vis spectra of the aforementioned four samples. The PEDOT:PSS sample showed a peak absorption at near 500 nm, however, the hydrogel's peak absorption occurred based on the dye that was in their synthesis process. The high salinity sample with red dye showed maximum absorbance at 534 nm which is due to the presence of red dyes. Green dyes in the cation-selective gel cause the maximum absorbance to be around 610 nm. The results match with the expectations.

The low salinity gel shows a maximum absorbance peak around 620 nm. This can be explained by the fact that the dyes used in this project are natural food dyes and these dyes are conjugated

compounds. The substance reflects the 430-480 nm range of the visible spectrum and based on the color wheel, the absorption range of this dye would be in the range of 590-630 nm. Moreover, cation-selective gel, high salinity, and low salinity gel showed relatively higher absorbance intensity at higher wavelengths in comparison with the PEDOT:PSS sample. Some reasons could be behind this observation. The first reason for the light-harvesting property of these hydrogels is due to the presence of 2-hydroxy-4′ -(2-hydroxyethoxy)-2-methylpropiophenone which has a conjugated system so, the π-π stacking in this component carries a part of light absorption. The second reason is that the presence of the dyes completely changes the absorption property of the hydrogels. The conjugated part of the dyes plays the role of photon absorption and the higher the degree of conjugation, the higher absorbance at the low energy spectrum. Another reason is the higher thickness of the hydrogel layers. As it was mentioned before, thickened layers absorb more hence, the 1.5 mm layer of hydrogel had higher absorbance than 300 μm PEDOT:PSS layer.

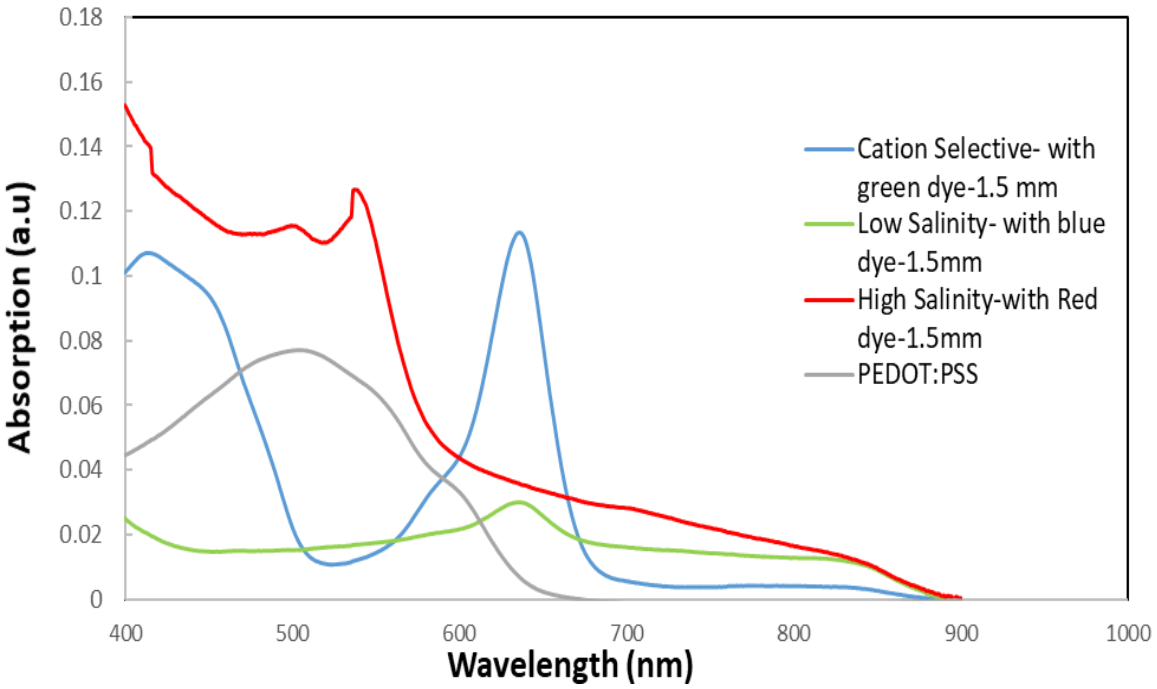

Figure 26 UV-Vis spectrum for the cation selective gel, low salinity gel, high salinity gel, and PEDOT:PSS.

The performance of any type of solar cell completely depends on the absorbance range of the cell. Also, the role of dyes in the absorption of light in these hydrogels is undeniable and the black dye has a varied range of absorbance among all colors. Therefore, we decided to improve the electric eel-inspired solar cell performance by using a black dye. Fig. 27 displays the comparison of the absorbance spectrum of high salinity gel with black dye and red dye. As it is expected, the hydrogel with black shows higher absorbance property.

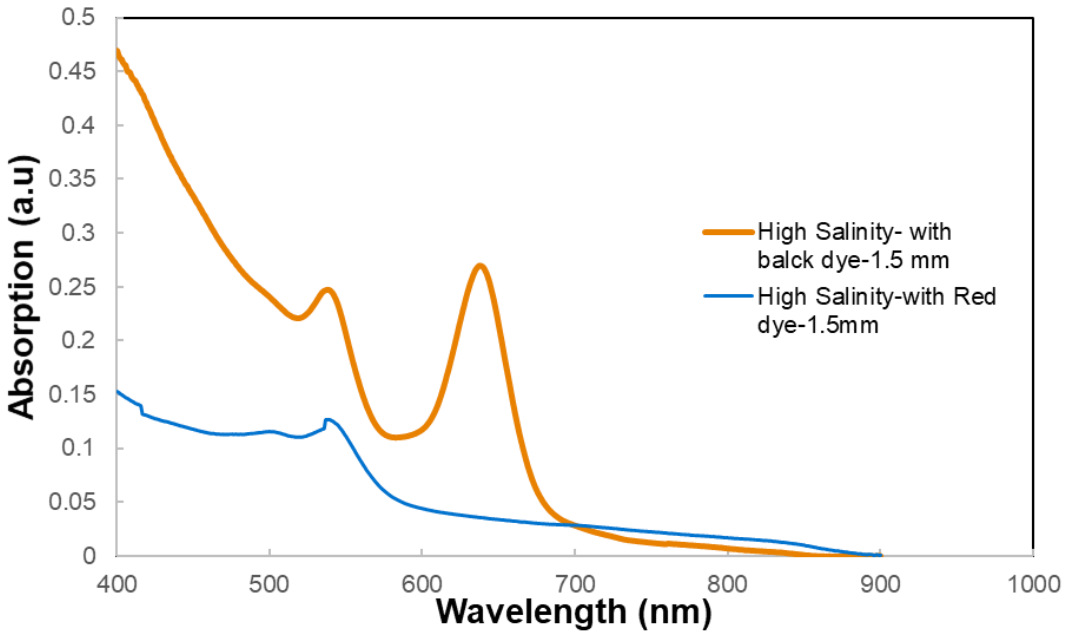

Figure 27 Absorption spectrum of high salinity gel with red dye and black dye with 1.5 mm thickness.

4.2.2 Photoconductivity Characterizations

The photoconductivity of the hydrogels and the electric eel-inspired solar cell with different structures are investigated in this section. After finding that these hydrogels have an amazing ability to harness light, charge transport, dissociation, and the collection part of the electric eel-inspired solar cell should be optimized to maximize the performance of the solar cell. Fig. 28 shows the I-V characteristics of the high salinity hydrogel and the low salinity hydrogels under irradiation and in dark. The graphs indicate that the photoconductivity of high salinity hydrogel is much higher than low salinity hydrogel. In this solar cell design, the high salinity gel acts as an active layer.

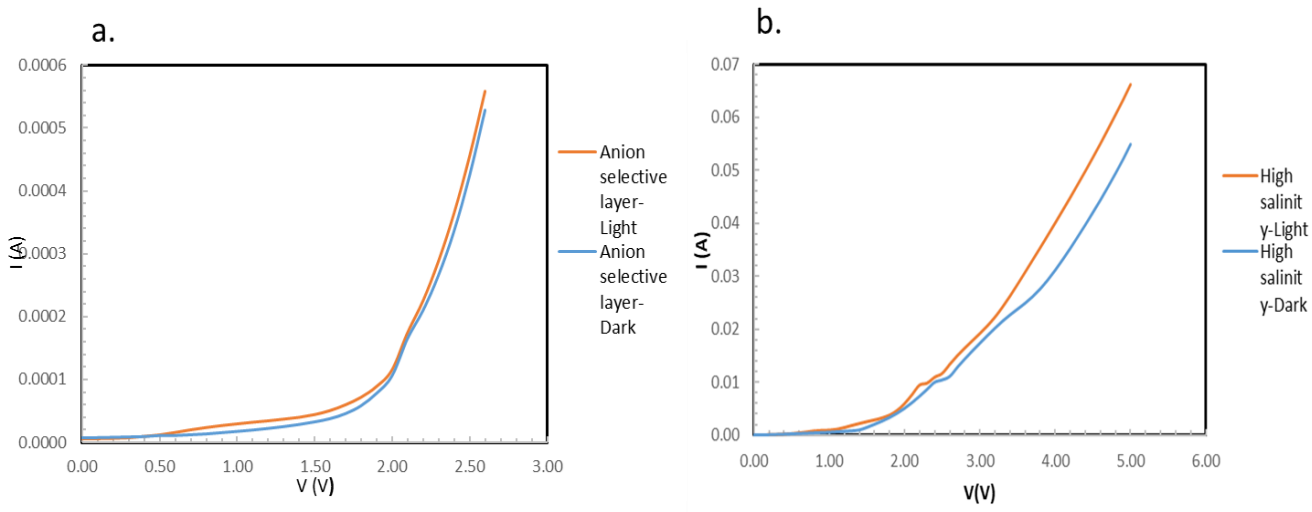

Figure 28 I-V characteristics of a. anion selective layer and b. high salinity hydrogels in dark and under irradiation

Fig. 29 shows the I-V characteristics of a two layer sample which consists of high salinity gel on top of a layer of low salinity gel. The sample under irradiation showed a current increase of about 12.2% at the source voltage of 2.5 V.

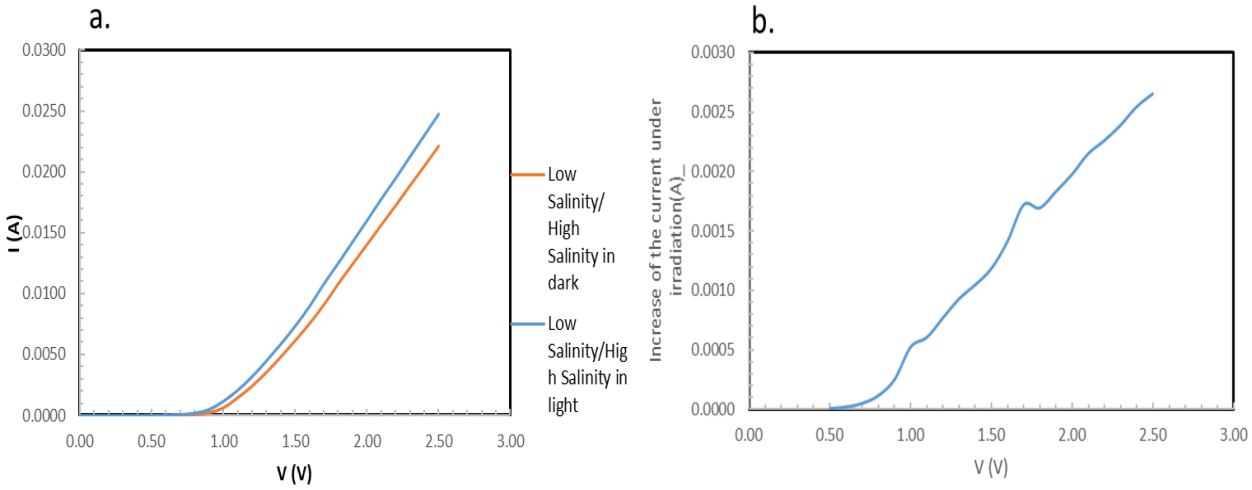

Figure 29 a. I-V characteristics of a. low salinity/high salinity hydrogels in dark and under irradiation, b. increase of current under irradiation

Fig. 30 compares the I-V characteristics of a three-layered sample which consists of a layer of high salinity hydrogel sandwiched between the anion-selective hydrogel and cation-selective hydrogel. The sample is photoconductive with 7% of current enhancement at the source voltage of 2.5 V.

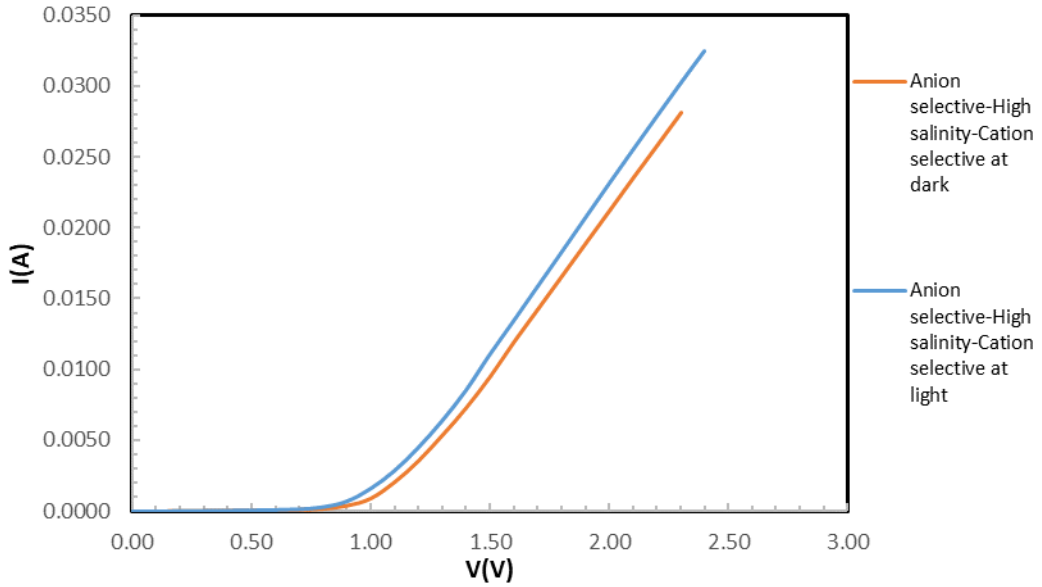

Figure 30 I-V characteristics of a three layered sample consisting of a layer of high salinity hydrogel sandwiched between anion-selective hydrogel and cation-selective hydrogel in dark and light.

Fig. 31 compares the I-V behavior of another three-layered sample consists of a high salinity hydrogel sandwiched between two layers of low salinity hydrogels. In this sample, a 59.9% current increase under light irradiation has been observed at a source voltage of 2.9 V. This observation can be explained by the fact that the high electromotive force of the ionic gradient in this sample added up to photocurrent generation in dyes. The osmosis effect generates a diffusion force for the

movement of free ions. Therefore, without any barriers of anionic and cationic, high ionic-concentration differences inherently generate an ionic current in the sample.

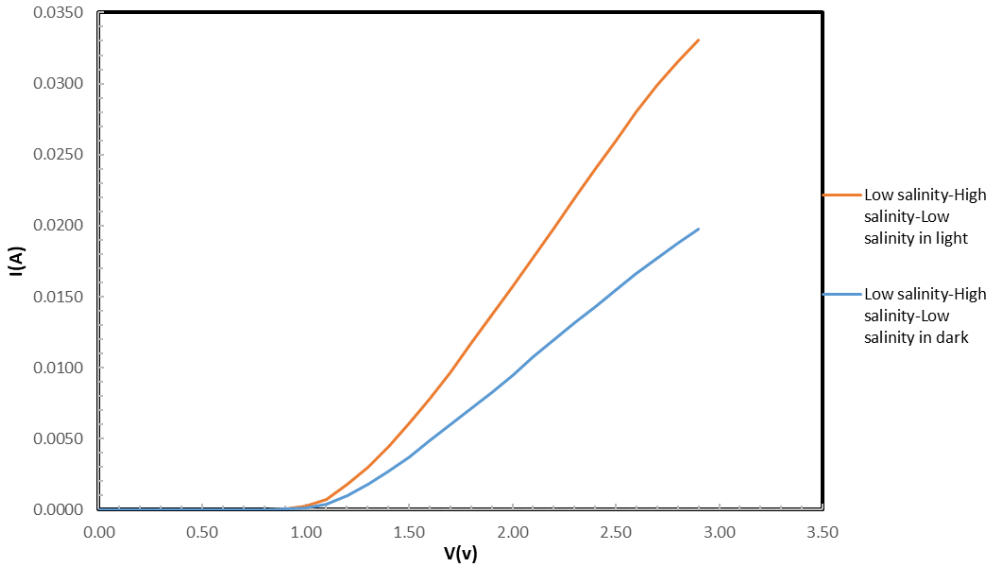

Figure 31 I-V behavior of another three layered sample consists of a high salinity hydrogel sandwiched between two layers of low salinity hydrogels in dark and light.

Lastly, Fig.32 shows the I-V characteristics of a five-layered sample including low salinity, anion-selective, high salinity, and cation-selective, and low salinity respectively. The current increase under irradiation begins after the source voltage of 1.5 V. Also, the amount of current is much less than 2 layered and 3 layered samples because of a lower amount of ionic components.

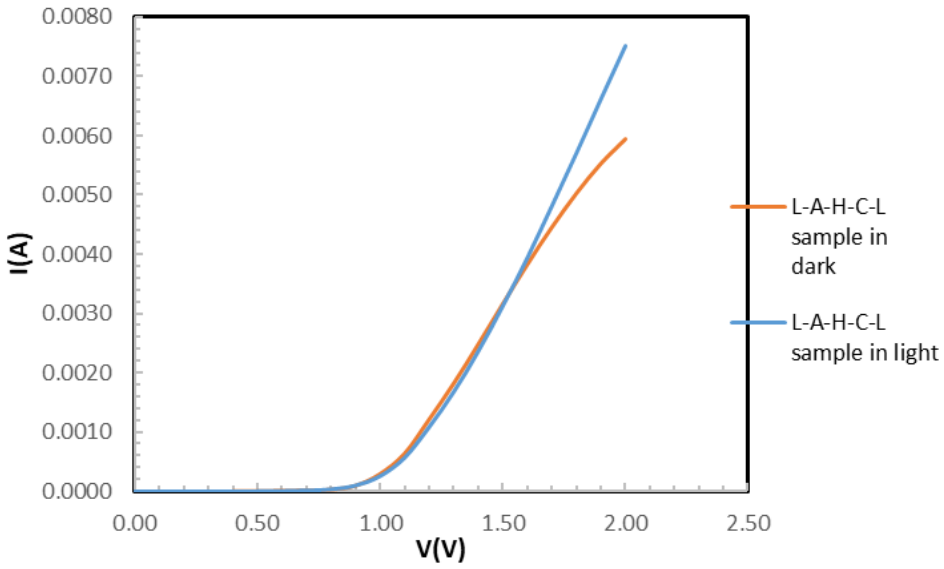

Figure 32 I-V characteristics of a five layered sample including low salinity, anion selective, high salinity, and cation selective, and low salinity respectively in dark and light.

4.2.3 Solar Simulator Results

The efficiency of the electric eel-inspired solar cell has been investigated for different configurations of layers. The first version mimics the artificial electrocyte structure and contains five layers of high salinity, cation-selective, low salinity, anion-selective, and high salinity hydrogels. Fig. 33 shows the I-V characteristics of this version under one sun irradiation. All of the tests have been conducted under total irradiance of A.M1.5 using a standard condition of 100 mW/cm^2 for 15 seconds (Solar Simulator 1000 Optical Radiation Corporation) and the I-V measurements have been done with a Keithley 2400 source meter. This version showed a power conversion efficiency of 3.13% and a short current density of 4.745 mA/cm^2. Osmotic force is from high salinity gel to low salinity gel so to improve the design, the high salinity gel must be in the middle of the layers.

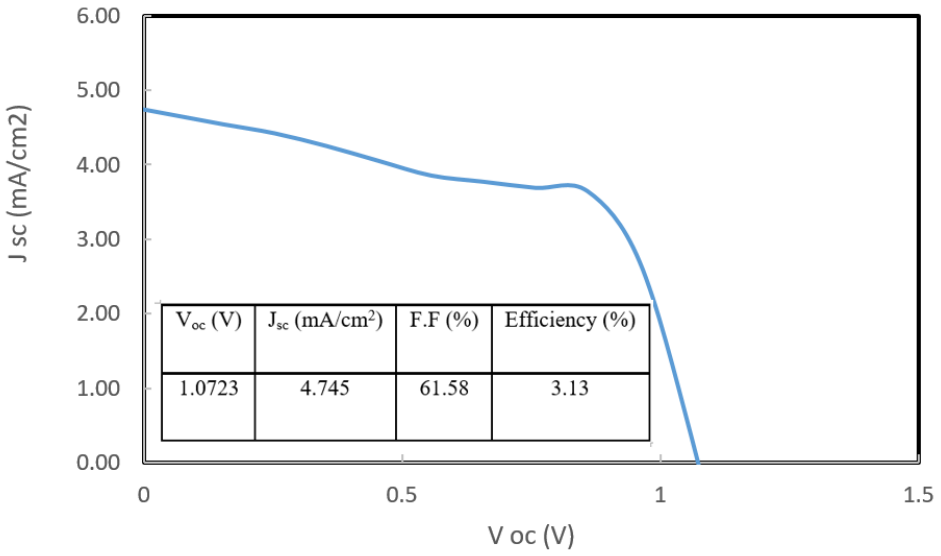

Figure 33 J-V characteristics of electric eel-inspired solar cell with five layers of high salinity, cation selective, low salinity, and anion selective, and high salinity hydrogels.

To improve the power conversion efficiency of the bio-inspired solar cell, different arrangements of layers have been implemented. The second version contains anion-selective, high salinity, and cation-selective gel. The power conversion efficiency was 3.37 which shows enhancement and the current density is 6.475 mA/cm^2. In this cell, high salinity gel acts as the active layer, and cation and anion-selective gels act as hole transport and electron transport layers which are positive and negative free ions here.

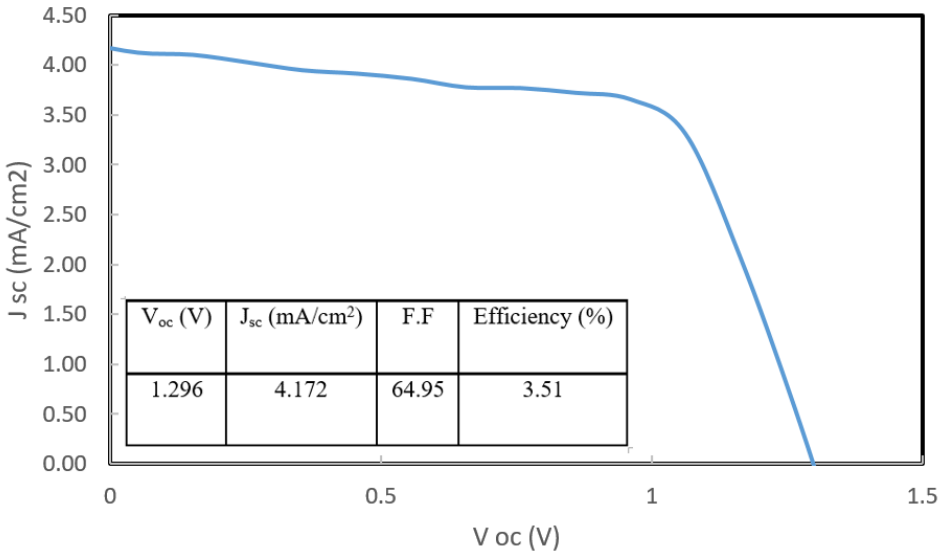

Figure 34 Characteristics of an electric eel-inspired solar cell with three layers of cation selective, high salinity, and anion selective hydrogels.

The next version of the eel-inspired solar cell contains three layers of low salinity, high salinity, and cation-selective hydrogel. This version showed 3.51 % power conversion efficiency and 4.172 mA/cm2 current density. The current density is less than the previous model because cation-selective and anion-selective hydrogels capture the negative and positive ions on opposite sides however, the fill factor of the L-H-C version is 18.24 % more than the C-H-A version so its efficiency is better. Fig. 35 shows the result of the L-H-C solar cell compared to the I-V characteristics of a dye-sensitized solar cell. Surprisingly, the electric-eel inspired solar cell shows fascinating results under sun irradiation and this proves that this type of solar cell could be a game-changing model in the future market of solar energy systems.

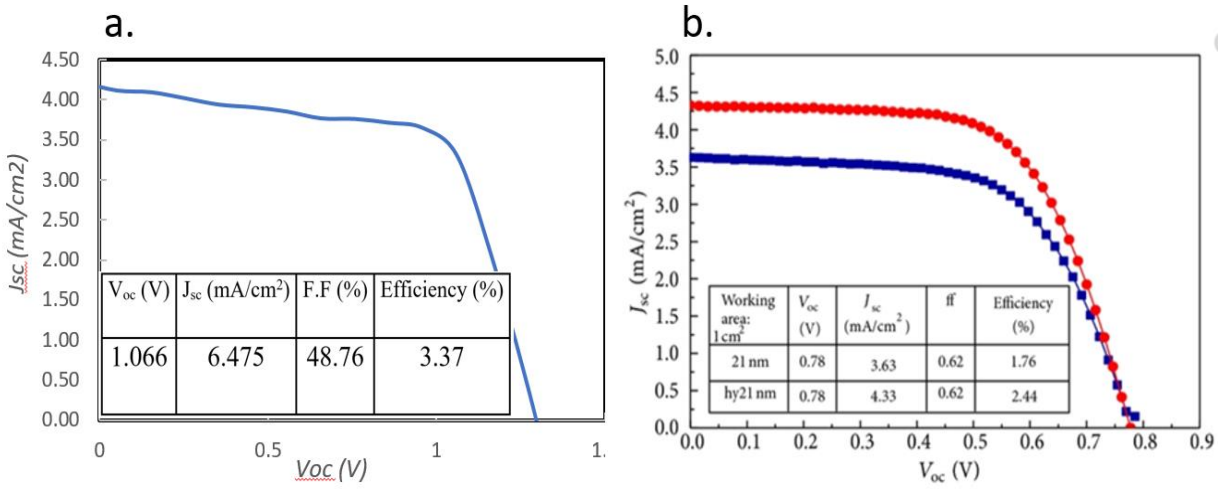

Figure 35 Characteristics of an electric eel-inspired solar cell with three layers of cation selective, high salinity, and low salinity hydrogels.

To obtain the impact of osmotic force under irradiation, characteristics of low salinity/high salinity two-layered solar cell have been investigated. The cell showed 3.47% power conversion efficiency which is 0.04% lower when there is a cation-selective gel layer. Fig. 36 shows the result for a two-layered solar cell. By adding a low salinity layer to this model, the efficiency reached 5.08%. Fig. 37 showed the I-V characteristics of the low salinity/high salinity/low salinity model. Ion concentration gradient generates an electromotive force between low salinity and high salinity layers in turn, the ions diffusion rate rises. On the other hand, adding cation and anion-selective hydrogel layers between low salinity and high salinity decreased the efficacy to 4.62%. The reason behind this result is that the recombination of free ions in two cation and anion-selective layers are reducing the photocurrent density. Fig. 38 shows the results for five-layered solar cell including low salinity, cation-selective, high salinity, and anion-selective, low salinity hydrogels.

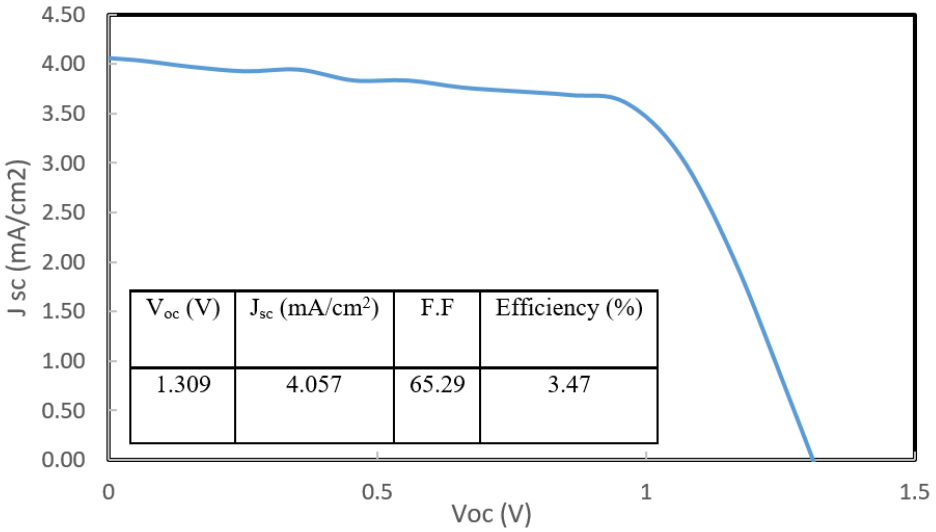

V_{oc} (V)	J_{sc} (mA/cm^2)	F.F	Efficiency (%)
1.309	4.057	65.29	3.47

Figure 36 Characteristics of an electric eel-inspired solar cell with two layers of high salinity and low salinity hydrogels.

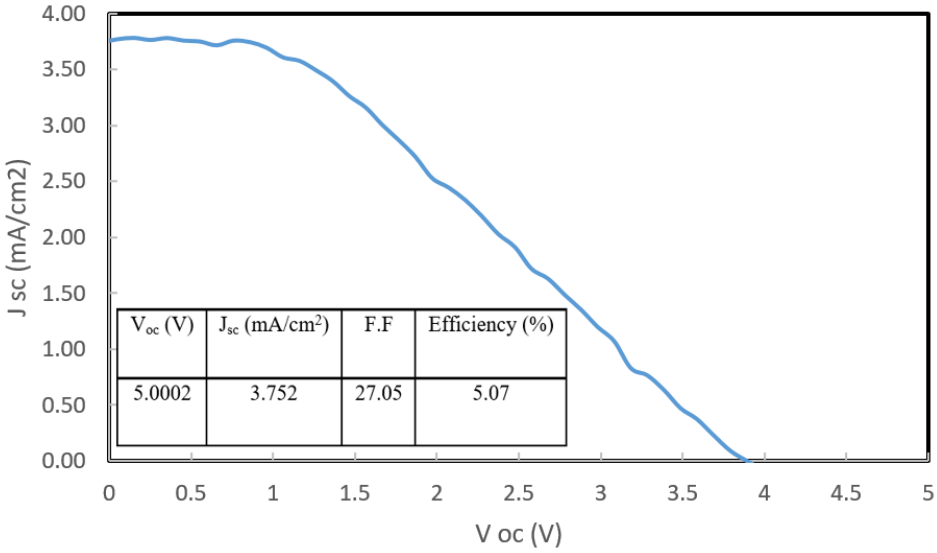

V_{oc} (V)	J_{sc} (mA/cm^2)	F.F	Efficiency (%)
5.0002	3.752	27.05	5.07

Figure 37 Characteristics of an electric eel-inspired solar cell with three layers of low salinity, high salinity, and low salinity hydrogels.

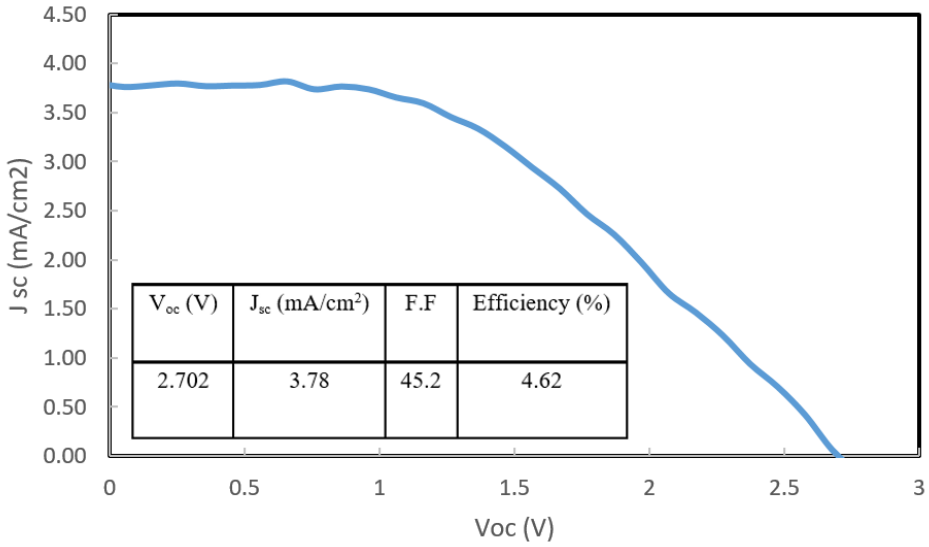

Figure 38 Characteristics of an electric eel-inspired solar cell with five layers of low salinity, cation selective, high salinity, and anion selective, and low salinity hydrogels.

In general, the sample with three layers of low/high/low salinity hydrogels showed 5.07 % power conversion efficiency. While the sample with cation and anion-selective layers showed the highest current density among all samples which can be explained by the fact that the cation and anion-selective layers act as a positive and negative ion transport layer. Table.3 provides the performance of the different devices under one sun irradiation.

Table 3. Performance of different versions of the electric eel-inspired solar cell

Cell arrangement	**V oc (V)**	**J sc (mA/cm^2)**	**Fill Factor (%)**	**Efficiency (%)**
L-H-L	5.0002	3.752	27.05	5.07
L-A-H-C-L	2.702	3.78	45.2	4.62
L-H	1.309	4.057	65.29	3.47
L-H-C	1.296	4.172	64.95	3.51

A-H-C	1.066	6.475	48.76	3.37
H-C-L-A-H	1.0723	4.745	61.58	3.13

Chapter 5

Conclusions and Future Prospects

5.1 Conclusion

One solution to satisfy ever-increasing global energy demands includes greatly enhanced and significantly more efficient solar energy collection and conversion systems [1]. In this project, we present a novel photovoltaic solar cell inspired by an electric eel with fascinating features such as cost efficiency, eco-friendliness, and ease of manufacturing which makes it a great candidate to fulfill the solar energy market demands. In addition, we introduced a new flexible, transparent, and low-cost PAM hydrogel material to the solar cells Integration of this PAM hydrogel material by our unique configuration of layers to generate a PV energy convertor is reported here for the first time in solar cell history. This new unique technology inspired by artificial electrocyte is developed to reduce the manufacturing cost, improve the environmental effects, and enhance the power conversion efficiency of the solar energy converter. This solar cell promotes great conversion efficiency in the collection, separation, and transport of electrons/holes using mobile ions with 5.08% of power conversion efficiency. Heterogeneous multi-layer polyacrylamide hydrogel is used to fabricate this unique solar cell to mimic the electrical eel electrocyte organ which uses the ionic gradient electromotive force to flow free ions through an external circuit. By synthesizing four types of PAM hydrogels, artificial electrocyte has been mimicked and showed 150-180 mV of different potentials which is comparable to the transcellular potential of actual electrocyte. 1.29 V have been obtained by 7 tetrameric cells in series and 7 μA have reported from 3 parallel stacked rows of three series cells. By increasing the thickness of the gels, the resistance

increases. We showed that by encapsulating the cells, their durability gets doubled. Integration of these hydrogels with natural dyes enhanced the light absorption property and combination of different colored layers, expand the absorbed wavelength range of the sunlight. Also, the high salinity gel with black dye showed a wide range of absorption spectrum with maximum absorbance around 630 nm and 540 nm. Photoconductivity tests indicate that the artificial electric eel in layers is capable of photo generation. By merging the principles of photovoltaic cells and the artificial electric electrocyte, a 5.08% power conversion efficiency was obtained from three layers including low salinity, high salinity, and low salinity hydrogel layers under one sun standard irradiation. Due to the osmotic force as well as the light-harvesting property of the layers, 6.475 mA/cm^2 has been captured for a three-layered solar cell with anion-selective/high salinity and cation-selective solar cell. The anion and cation-selective gels act as electron and hole transfer layers in conventional solar cells.

In summary, we successfully developed a new generation of photovoltaic solar cells that shows a commercially realistic power conversion efficiency, made from low-cost eco-friendly materials using a very cost-efficient fabrication technique for the first time in the world. This cell has a great potential to be a game-changer in the solar cell market due to its fascinating features such as semi-transparency, low manufacturing cost, and being environmentally friendly.

5.2 Future Prospects

A completely new generation of solar photovoltaic cells has been proposed in this thesis. No one can deny that the fascinating mechanism of the ionic energy pathway in this solar cell can be implemented in sustainable systems to enhance the performance of energy conversion. To mimic

the electrocyte organ in detail, some alternative strategies can be used. For example, by printing the gels on a pre-patterned substrate, the thickness of the gels will drop down in turn, and the conductivity of the artificial eel will be enhanced. Another strategy is using foldable sheets which makes it possible for the artificial electrocyte to be used in batteries. To improve the efficiency of the electric eel-inspired solar cell, utilizing light absorber nanomaterials such as PEDOT:PSS could be an interesting idea to enhance the light absorption property of the cell. Moreover, using ITO transparent electrode instead of Al electrodes will increase the light intensity reaches the hydrogel as well as improving the ion mobility and collection. Improving the fabrication method and merging the fabrication with an additive manufacturing system would be an interesting idea to focus on. Research on solar cells continues to increase and new developments in bio-inspired systems are published every day. A new area of exploration in solar cells may be born around the ion gradient energy transfer pathway. This ever-expanding pool of research shows that solar energy is a viable resource to sustain human energy demands and brings hope that there may be a solution to our current energy crisis. Accordingly, it should be noted that the next technological advancement in any field may stem from what already exists and there are surely many natural masterpieces in the world waiting to be explored and appreciated.

Bibliography

[1] N. Soudi, S. Nanayakkara, N. M. S. Jahed, and S. Naahidi, “Rise of nature-inspired solar photovoltaic energy convertors,” *Sol. Energy*, vol. 208, no. May, pp. 31–45, 2020, doi: 10.1016/j.solener.2020.07.048.

[2] M. J. Menne, C. N. Williams, B. E. Gleason, J. Jared Rennie, and J. H. Lawrimore, “The Global Historical Climatology Network Monthly Temperature Dataset, Version 4,” *J. Clim.*, vol. 31, no. 24, pp. 9835–9854, 2018, doi: 10.1175/JCLI-D-18-0094.1.

[3] H. Zhou *et al.*, “Bio-Inspired Photonic Materials: Prototypes and Structural Effect Designs for Applications in Solar Energy Manipulation,” *Adv. Funct. Mater.*, vol. 28, no. 24, pp. 1–27, 2018, doi: 10.1002/adfm.201705309.

[4] T. M. Razykov, C. S. Ferekides, D. Morel, E. Stefanakos, H. S. Ullal, and H. M. Upadhyaya, “Solar photovoltaic electricity: Current status and future prospects,” *Sol. Energy*, vol. 85, no. 8, pp. 1580–1608, 2011, doi: 10.1016/j.solener.2010.12.002.

[5] R. Singh and H. W. Rhee, “The rise of bio-inspired energy devices,” *Energy Storage Mater.*, vol. 23, pp. 390–408, 2019, doi: 10.1016/j.ensm.2019.04.030.

[6] F. Odobel, Y. Pellegrin, and J. Warnan, “Bio-inspired artificial light-harvesting antennas for enhancement of solar energy capture in dye-sensitized solar cells,” *Energy Environ. Sci.*, vol. 6, no. 7, pp. 2041–2052, 2013, doi: 10.1039/c3ee24229c.

[7] C. Yang and Z. Suo, “Hydrogel ionotronics,” *Nat. Rev. Mater.*, 2018, doi: 10.1038/s41578-018-0018-7.

[8] T. B. H. Schroeder *et al.*, “stacked hydrogels,” *Nat. Publ. Gr.*, 2017, doi: 10.1038/nature24670.

[9] J. Xu and D. A. Lavan, “Designing artificial cells to harness the biological ion concentration gradient,” vol. 3, no. November, 2008, doi: 10.1038/nnano.2008.274.

[10] L. Han, X. Lu, M. Wang, D. Gan, W. Deng, and K. Wang, “A Mussel-Inspired Conductive , Self-Adhesive , and Self-Healable Tough Hydrogel as Cell Stimulators and Implantable Bioelectronics,” pp. 1–9, 2016, doi: 10.1002/smll.201601916.

[11] A. Polman, M. Knight, E. C. Garnett, B. Ehrler, and W. C. Sinke, “Photovoltaic materials: Present efficiencies and future challenges,” *Science (80-.).*, vol. 352, no. 6283, 2016, doi:

10.1126/science.aad4424.

[12] M. R. Matthews, “Science and worldviews in the classroom: Joseph Priestley and photosynthesis,” *Sci. Educ.*, vol. 18, no. 6–7, pp. 929–960, 2009, doi: 10.1007/s11191-009-9184-8.

[13] D. A. Cusano, “CdTe solar cells and photovoltaic heterojunctions in II-VI compounds,” *Solid State Electron.*, vol. 6, no. 3, pp. 217–232, 1963, doi: 10.1016/0038-1101(63)90078-9.

[14] G. Magiels, “Dr Jan IngenHousz , or why don ’ t we know who discovered photosynthesis ?,” vol. 1, no. November, pp. 15–17, 2007.

[15] B. O’Regan and M. Grätzel, “A low-cost, high-efficiency solar cell based on dye-sensitized colloidal TiO2 films,” *Nature*, vol. 353, no. 6346, pp. 737–740, 1991, doi: 10.1038/353737a0.

[16] J. Gong, C. Li, and M. R. Wasielewski, *Advances in solar energy conversion*, vol. 48, no. 7. 2019.

[17] N. M. Haegel *et al.*, “Terawatt-scale photovoltaics: Transform global energy,” *Science (80-.).*, vol. 364, no. 6443, pp. 836–838, 2019, doi: 10.1126/science.aaw1845.

[18] P. K. Nayak, S. Mahesh, H. J. Snaith, and D. Cahen, “Photovoltaic solar cell technologies: analysing the state of the art,” *Nat. Rev. Mater.*, vol. 4, no. 4, pp. 269–285, 2019, doi: 10.1038/s41578-019-0097-0.

[19] E. Shi *et al.*, “Improvement of graphene-Si solar cells by embroidering graphene with a carbon nanotube spider-web,” *Nano Energy*, vol. 17, pp. 216–223, 2015, doi: 10.1016/j.nanoen.2015.08.018.

[20] S. Lou, X. Guo, T. Fan, and D. Zhang, “Butterflies: Inspiration for solar cells and sunlight water-splitting catalysts,” *Energy Environ. Sci.*, vol. 5, no. 11, pp. 9195–9216, 2012, doi: 10.1039/c2ee03595b.

[21] S. K. Hau, H. L. Yip, and A. K. Y. Jen, “A review on the development of the inverted polymer solar cell architecture,” *Polym. Rev.*, vol. 50, no. 4, pp. 474–510, 2010, doi: 10.1080/15583724.2010.515764.

[22] S. V. Gaponenko, P. M. Adam, D. V. Guzatov, and A. O. Muravitskaya, “Possible nanoantenna control of chlorophyll dynamics for bioinspired photovoltaics,” *Sci. Rep.*, vol. 9, no. 1, pp. 1–14, 2019, doi: 10.1038/s41598-019-43545-4.

[23] G. Williams, Q. Wang, and H. Aziz, “The photo-stability of polymer solar cells: Contact photo-

degradation and the benefits of interfacial layers," *Adv. Funct. Mater.*, vol. 23, no. 18, pp. 2239–2247, 2013, doi: 10.1002/adfm.201202567.

[24] "S1364032117315526." .

[25] Y. Zou *et al.*, "sensing and energy harvesting," no. 2019, pp. 1–10, doi: 10.1038/s41467-019-10433-4.

[26] L. Han *et al.*, "Mussel-Inspired Adhesive and Conductive Hydrogel with Long-Lasting Moisture and Extreme Temperature Tolerance," vol. 1704195, pp. 1–12, 2018, doi: 10.1002/adfm.201704195.

[27] "B IOELECTRICITY INSPIRED POLYMER ELECTROLYTE MEMBRANES FOR," no. December, 2018.

[28] Sun, H., Fu, X., Xie, S., Jiang, Y. and Peng, H. (2016), Electrochemical Capacitors with High Output Voltages that Mimic Electric Eels. Adv. Mater., 28: 2070-2076. https://doi.org/10.1002/adma.201505742

[29] Y. Zhou, C. Wan, Y. Yang, H. Yang, S. Wang, and Z. Dai, "Highly Stretchable , Elastic , and Ionic Conductive Hydrogel for Artificial Soft Electronics," vol. 1806220, pp. 1–8, 2019, doi: 10.1002/adfm.201806220.

[30] C. Hu, Y. Zhang, X. Wang, L. Xing, L. Shi, and R. Ran, "Stable , Strain-Sensitive Conductive Hydrogel with Antifreezing," 2018, doi: 10.1021/acsami.8b15287.

[31] Schroeder, T. B., Guha, A., Lamoureux, A., VanRenterghem, G., Sept, D., Shtein, M., ... & Mayer, M. (2017). An electric-eel-inspired soft power source from stacked hydrogels. Nature, 552(7684), 214-218.

[32] I. A. Physiology, "Introductory Animal Physiology."

[33] E. Organ, B. Heidelberg, L. N. York, B. Heidelberg, N. York, and P. Alegre, "Electric Organ," pp. 1050–1056.

[34] C. Number, "Acrylamide and Bis-Acrylamide Solutions Instructions for Use," no. 161, 2000.

[35] Z. Wu, X. Yang, and J. Wu, "Conductive Hydrogel- and Organohydrogel-Based Stretchable Sensors," 2020, doi: 10.1021/acsami.0c21841.

[36] S. Bashir *et al.*, "Fundamental Concepts of Hydrogels: Synthesis, Properties, and Their

Applications," *Polymers* , vol. 12, no. 11. 2020, doi: 10.3390/polym12112702.

[37] K. Xiao, L. Jiang, and M. Antonietti, "Ion Transport in Nanofluidic Devices for Energy Harvesting," *Joule*, vol. 3, no. 10, pp. 2364–2380, 2019, doi: 10.1016/j.joule.2019.09.005.

[38] C. Wan, K. Xiao, A. Angelin, M. Antonietti, and X. Chen, "The Rise of Bioinspired Ionotronics," vol. 1900073, 2019, doi: 10.1002/aisy.201900073.

[39] "S0079670018301965." .

[40] P. Schexnailder and G. Schmidt, "Nanocomposite polymer hydrogels," pp. 1–11, 2009, doi: 10.1007/s00396-008-1949-0.

[41] Q. Han, "materials Preparation of shape-controlled electric-eel-inspired SnO 2 @ C anode materials via SnC 2 O 4 precursor approach for energy storage," *J. Mater. Sci.*, vol. 55, no. 25, pp. 11524–11534, 2020, doi: 10.1007/s10853-020-04752-x.

[42] T. Distler and A. R. Boccaccini, "Acta Biomaterialia 3D printing of electrically conductive hydrogels for tissue engineering and biosensors – A review," *Acta Biomater.*, vol. 101, pp. 1–13, 2020, doi: 10.1016/j.actbio.2019.08.044.